Journal of Structural Geology 33 (2011) 1728–1750

Contents lists available at SciVerse ScienceDirect

Journal of Structural Geology

journal homepage: www.elsevier.com/locate/jsg

Review article

The role of second phases for controlling microstructural evolution in polymineralic rocks: A review

M. Herwegh[a,*], J. Linckens[a,1], A. Ebert[a], A. Berger[a,b], S.H. Brodhag[a]

[a] Institute of Geological Sciences, University of Bern, Baltzerstrasse 1+3, 3012 Bern, Switzerland
[b] Institute for Geography and Geology, Copenhagen Universitet, Denmark

ARTICLE INFO

Article history:
Received 17 November 2010
Received in revised form
18 August 2011
Accepted 31 August 2011
Available online 22 September 2011

Keywords:
Zener pinning
Second phase
Grain coarsening
Deformation

ABSTRACT

We present a state-of-the-art review of the microstructural evolution in rocks under static and deformational conditions. First, the general concepts and processes are introduced using monomineralic aggregates. Then, they are expanded into the more complex context of polymineralic rocks with a dominant matrix phase. The first part of this contribution delivers information on sample strategies to quantify polymineralic microfabrics. Based on comparisons between microfabrics of monomineralic and polymineralic rocks, we use the common knowledge collected over the past decades for monomineralic systems and discuss the differences to polymineralic ones in terms of microstructures, modal compositions, spatial distribution of phases, crystallographic preferred orientations and associated processes. The article puts particular emphasis on the effect of coupled grain growth, mass transfer processes, and deformation mechanisms. We speculate on the effect of mineral reactions during the evolution of microstructures and rheology in polymineralic aggregates at different metamorphic conditions. At the end of the article, we demonstrate the great potential of grain-size evolution maps as microstructural tool to unravel the geological history of polymineralic rocks that evolved under a variety of geodynamic situations.

1. Introduction

Natural microstructures of rocks are of great importance since they, if stabilized and preserved, provide important information on the physical and chemical conditions during different stages of their evolution (e.g., Handy, 1987, 1989; Bestmann et al., 2000; Jessell et al., 2003; Pearce and Wheeler, 2010). The capability of reading both monomineralic and polymineralic microstructures is therefore crucial to unravel a rock's evolution, allowing the detection of deformation and/or thermal histories (e.g., Ramsay, 1967; Means, 1976; Fischer and Woodward, 1992; Vernon, 2004). In this light, the quantitative analysis of microstructures is paramount including a parameterization of grain sizes, grain-size distributions (also referred to as crystal-size distributions: CSD), SPO (shape-preferred orientation), as well as the spatial distribution of phases. Particularly, grain size plays a fundamental role in this context (Twiss, 1977; Frost and Ashby, 1982; ter Heege et al., 2002). When also CPO (crystallographic preferred orientation) is included in the description, the aggregates are referred to as microfabrics (see Schmid and Handy, 1991). To understand micro-scale processes involved in rock deformation, special attention has been paid to the study of monomineralic aggregates in the early days of microstructural research from an experimental and natural point of view (e.g., Voll, 1960; Hobbs, 1966; Guillopé and Poirier, 1979). In the past decades, an increasing number of investigations dealt with the more complex evolution of polymineralic rocks, a crucial step, given the fact that more than 95 vol.-% of rocks are polymineralic (Burg and Wilson, 1987; Jordan, 1987; Tullis et al., 1991; Handy, 1994; Berger and Stünitz, 1996; Fliervoet and White, 1995; Herwegh and Jenni, 2001; Ji et al., 2001, 2003; Berger and Herwegh, 2004; Barnhoorn et al., 2005b; Dimanov and Dresen, 2005; Ebert et al., 2007a,b; Delle Piane et al., 2009; Wilson et al., 2009; Fusseis et al., 2009; Brodhag and Herwegh, 2010; Linckens et al., 2011a,b).

One approach to parameterize polymineralic rocks is the determination of the volume fractions of different rheological phases (e.g., Handy, 1990; Song and Ree, 2007). Although being successfully applied to partially molten systems (e.g., Rosenberg and Handy, 2005), severe limitations arise because of lacking

* Corresponding author.
E-mail addresses: Herwegh@geo.unibe.ch, marco.herwegh@geo.unibe.ch (M. Herwegh).
[1] Now at: Department of Earth and Planetary Sciences, Washington University in St. Louis, 1 Brookings Drive, CB 1169, St. Louis, MO 63130, USA.

0191-8141/$ – see front matter © 2011 Elsevier Ltd. All rights reserved.
doi:10.1016/j.jsg.2011.08.011

information on geometrical aspects like the spatial distribution and interconnectivity of the different phases, their grain sizes or the percolation of fluids/melts through the aggregates (Zu et al., 2011). Such information is mandatory for establishing a proper link between microfabric and resulting rheology (e.g., Handy, 1990, 1992; 1994).

By using nature as a laboratory, we use selected samples to demonstrate how the aforementioned parameters can be measured in microfabrics, allowing microstructural quantification in a reliable manner. The general processes are introduced by focusing first on nearly monomineralic aggregates expanding then into the more complex interactions in the case of polymineralic aggregates. We will introduce some concepts on the base of monomineralic aggregates and expand them to polymineralic rocks using carbonates and peridotites as two prominent representatives of crustal and mantle rocks. The principles presented, however, do apply for all polymineralic microfabrics with a volumetrically dominant matrix phase.

2. Meso- to large-scale investigations

Large-scale deformation is controlled by microstructural processes, which are driven by minimization of internal free energy owing to changes in physico-chemical conditions, for example temperature, strain, flow stress/strain rates and chemical potentials (e.g., Regenauer-Lieb and Yuen, 2003; Herwegh and Berger, 2004). To learn more about the link between microfabric and meso- to large-scale structures two approaches have been followed in the past: (i) studies on the meso-scale (several meters to tens of meters) and (ii) investigations on the large-scale (kilometers).

(i) Particularly the study of meso-scale structures, like shear zones, is appealing, because often strain gradients along and across shear zones can be used in the sense of Means (1995) to infer the evolution of microstructures with increasing shear strain (Ramsay, 1980; White et al., 1980; Hudleston, 1980; Watts and Williams, 1983; Fusseis et al., 2006; Warren and Hirth, 2006; Oesterling et al., 2007; Toy et al., 2009; Schrank et al., 2008; Skemer et al., 2010). However, the study of meso-scale structures faces the problems of the estimation of absolute deformation temperatures and potential retrograde reactivation. Also, information on the time interval of the activity of such small and short-lived structures is critical but would be mandatory to unravel strain rates and to learn more about the associated process rates (Schrank et al., 2008).

(ii) Studies on large-scale structures can deliver more reliable information (large-scale shear zones, contact metamorphic aureoles, regional metamorphism) by combining information on gradients in temperature, shear strain or strain rate with corresponding sampling strategies. Despite some uncertainties of some of these parameters, large sample series along the structures will result in statistically robust datasets on relative changes of these parameters, because potential local variations and uncertainties will be cancelled out (Handy, 1987; Dunlap et al., 1997; Stipp et al., 2002b; Herwegh and Pfiffner, 2005; Ebert et al., 2008; Toy et al., 2008). On the kilometer-scale, pronounced temperature gradients can be unraveled using different geothermometers, which can result in reliable temperature estimates (Herwegh and Berger, 2003; Herwegh and Pfiffner, 2005; Ebert et al., 2008; Grujic et al., 2009; Linckens et al., 2011a). In large-scale shear zones, sampling profiles along the transport direction allows to track down microstructural variations as a function of changing temperature, stress and strain rate conditions representing a field laboratory in which the processes can directly be compared to experimental and theoretical data (e.g., Dunlap et al., 1997; Stipp et al., 2002a; Herwegh et al., 2005b; Mehl and Hirth, 2008). In the ideal case, knowledge of the total displacement, the shear zone width and the time interval of deformation may allow the calculation of strain rates. Even with the common uncertainties related to the time interval of deformation, at least the order of strain-rate magnitude can be obtained by following this strategy. Ideally, such sample series are accomplished by sample profiles across the shear zones, by which potential shear gradients or the retrograde shrinkage of the shear zone may become visible (e.g., Herwegh and Pfiffner, 2005; Ebert et al., 2007b; Austin et al., 2008; Herwegh et al., 2008).

3. Quantitative description of microfabrics

The proper description of microfabrics requires not only the grain sizes and the abundance of the different phases but also information on their chemical compositions, spatial distributions and geometric relationships (e.g., Turner and Weiss, 1963; Jerram et al., 1996; Jerram and Higgins, 2007). Since these parameters can vary laterally in a substantial manner, a definition of microstructural *R*epresentative *E*lementary *V*olume (REV) is required (e.g., Schrank et al., 2008; Liu et al., 2009), where the sizes, abundance and distributions of the phases can be considered to be constant. From a statistical point of view, the REV must be large enough to cover a couple of hundred grains. Therefore, quantitative descriptions of different REV are mandatory, requiring the application of automated analysis techniques. At first glance, picking the REV by eye is a valid approach because human's inspection is rather efficient. During data processing, the statistical relevance has to be evaluated in terms of each individual data set per REV but also for the overall database. In this work, mineral type, size, aspect ratio, perimeter, orientation, volume fraction and grain center of each individual grain were quantified for all phases with image analysis software (Berger et al. this volume). Based on these measurements, area- and number-weighted grain-size distributions, volume fractions of the different phases, grain-shape preferred orientations and nearest-neighbor relationships can be obtained. The geometrical spacing of phases is crucial, because it contributes to how and at which rate chemical processes can occur and over which distances mechanical responses due to the presence of a specific phase are expected to occur. In this sense, the selection and definition of REV is rather crucial allowing the discrimination of chemically or mechanically variable microstructures. Note that in the entire review we restrict to the 2D space, leaving space for future studies in the more complex 3D world (Fusseis et al., 2009; Zu et al., 2011; Berger et al., this volume).

4. Spatial distribution of mineral phases and their presentation in the Zener space

In a polymineralic rock with dominant matrix phase (matrix phase volume fraction > 0.5), the occurrence of chemical impurities and/or other minerals, the so-called second phases, will influence different physico-chemical processes. These processes are subdivided into those acting at interfaces between matrix mineral and second phase, or those affecting solely the matrix phase. The resulting "bulk" microstructure, especially the stable grain size in the case of mylonites, represents the balance between grain-size reduction and grain growth, i.e. reflect a microstructural equilibrium (Herwegh and Berger, 2004; Austin and Evans, 2007, 2009). In all examples with initial grain sizes below the equilibrium grain size, the grain boundary mobility will influence the way and the

rate at which the equilibrium grain size is approached. Grain boundary mobility is controlled by temperature conditions and mechanical and chemical influences. The second-phase particles, for example, affect the grain boundary velocity (V) by imposing drag forces (F_{drag}) on the moving matrix grain boundaries, which counteract the driving forces in the following manner:

$$V = M \cdot \left(F - F_{drag}\right) \quad (1)$$

where F is the driving force for grain boundary migration, which is based on potentials of surface energy, chemical compositions or internal strain energy (dislocation density). M is the grain boundary mobility (see Fig. 4 in Evans et al., 2001). F_{drag} directly relates to size and shape of the second-phase particle: large or ellipsoidal particles impose larger dragging forces on a moving grain boundary than small or spherical ones (see Gladman, 1966; Manohar et al., 1998; Nes et al., 1985; Ryum et al., 1983; Smith, 1948 and review in Evans et al., 2001). As long as F_{drag} is smaller than F, the grain boundary will migrate, but with reduced velocity. It will be pinned once F_{drag} becomes equal or larger than F. Fig. 1 illustrates different examples of grain boundary pinning by micro-scale (a-d) and nano-scale particles (e) as well as by atomic solutes at grain boundaries (f). Note that, particularly in the case of nano-scale particles and solute impurities, the drag force of an individual particle is rather limited at the first instant leading to increased drag by particle accumulation as the grain boundary moves (see Fig. 1e). Consequently, F_{drag} increases steadily. Once the bulk F_{drag} becomes larger than F, the grain boundary can be immobilized even by such small-sized particles. Solute drag, i.e. changes in grain boundary mobility by impurity atoms (Cahn, 1962), can also be induced by the segregation of atoms in grain boundaries. This affects mineral aggregates in which solid-solutions are observed (e.g., Davies et al., 2010; Freund et al., 2001; Herwegh et al., 2003). Prominent examples of pinning by nanoparticles are all rock types with an originally small matrix grain size such as impure micritic limestones (Berger and Herwegh, 2004) or cherts (Okudaira et al., 2010).

In nature, polymineralic rocks often contain second phases that have a size of a few microns and larger, reaching up to the size of the matrix grains. In these cases, the spacing of the second-phase minerals defines the maximum distance over which a matrix grain can grow until its boundaries become completely pinned by second phases. Fig. 2 illustrates the relation between the spacing of the second phases and the corresponding matrix grain size for three carbonate mylonites deformed at different temperatures with mono- (left column) and polymineralic layers (right column). While the left column shows the distribution of the intergranular distances between the five nearest neighbors of grains in mono-mineralic mylonitic aggregates, the right column displays both the interparticle distances for the second-phases (red), and the matrix (yellow). It is evident that the mean spacing of the mica directly controls the mean interparticle distance of the calcite grains, which correlates with the calcite's grain size. The ratio of the mean value of the interparticle spacing of the second phase to the one of the matrix grains, K, allows determination of the degree of pinning. While $K < 1$ characterizes microstructures with large-second phase spacing, $K > 1$ indicates fully pinned matrix grains (Fig. 2). Only second phases at matrix grain boundaries can be used for this consideration (Brodhag and Herwegh, 2010). Variations in the interparticle distances of second phases and the corresponding effect on the matrix grain size is typical for many polymineralic rocks and has also been found in material sciences (e.g., see fig. 3.29 in Passchier and Trouw, 2005; Fig. 5 in Krabbendam et al., 2003; Fig. 1 in Brodhag and Herwegh, 2010). In the latter case, Zener (in Smith, 1948) suggested a simple mathematical relation, which expresses the maximum matrix grain size (D_{max}) as a function of the size (d_p) and volume fraction (f_p) of the second phases:

$$D_{max} = c \cdot d_p / f_p \quad (2)$$

where c is a constant. The ratio d_p/f_p is also referred to as the Zener parameter or Zener ratio, Z (e.g., Herwegh and Berger, 2004). For a given second-phase grain size, small Z values characterize polymineralic rocks with a large volume fraction of second phases, where the corresponding mean interparticle distance is small resulting in a small matrix grain size (Fig. 3 top). In contrast, high Z values typically reflect the monomineralic parts with large grain sizes (Fig. 3 bottom, see also discussion below).

In the field of material sciences, this equation was modified in different ways (see Table 2 in Manohar et al., 1998), for example taking into account the location of second phases on a grain boundary. Therefore, Eq. (2) is commonly modified by a geometric parameter "m" as exponent to f_p:

$$D = c \cdot d_p / f_p^m \quad (3)$$

If second phases are small and distributed homogeneously, m assumes a value of unity. For $m = 0.5$, second phases sit between grain triple junctions on grain boundaries. If they are located at grain triple junctions, m is 0.33 (see references in Evans et al., 2001). m is the slope of the linear best fit of a $\log(d_p/D)$ over $\log(f_p)$ plot (Fig. 4a). In polymineralic rocks, m varies between 0.24 and 0.59 (Table 1).

Pinning at grain triple junctions could be inferred from m values around 0.33. However, in nature, second-phase particles do not strictly follow this geometric arrangement but are in fact found at any grain boundary location as well as within grains. Among other parameters like non-uniform size or shape of the particles, it is this spatial scattering which causes the data scatter in Fig. 4a. When presenting the data in $\log(D)$ versus $\log(d_p/f_p^m)$ space (Fig. 4b), it becomes evident that the scatter is not arbitrary, but follows pre-defined predictable trends, showing an increase in D with increasing d_p/f_p^m at low values and a constant D at higher values. This trend demonstrates that the use of m values in Eq. (3) results in a collapse of the data along the x-axis in comparison to Eq. (2) (compare Fig. 4b with c, see also Ebert et al. 2008). Consequently, it is difficult, if not even impossible, to discriminate different microstructural dependencies in terms of second-phase effects and dynamic recrystallization controlled behavior (see below). We therefore resort to the application of the original Zener ratio (Eq. (2)), well knowing that we disregard the geometric relation in this way. This approach yields the following modified version of the Zener equation (eq. (4)):

$$D = c \cdot \left(d_p / f_p\right)^{m^*} \quad (4)$$

where m^* is now the exponent of the entire Zener ratio. In contrast to m (slope in Fig. 4a), m^* represents the slope of the trend lines in Fig. 4c.

5. Microstructural evolution under static conditions

5.1. Grain growth and coarsening processes under contact metamorphic conditions

At lithostatic pressure, i.e., under absent to small deviatoric stresses, and chemical equilibrium, reduction in surface energy by grain growth is the main energy-minimizing process in mono-mineralic aggregates (e.g., Joesten, 1983, 1991; Karato, 1989; Covey-

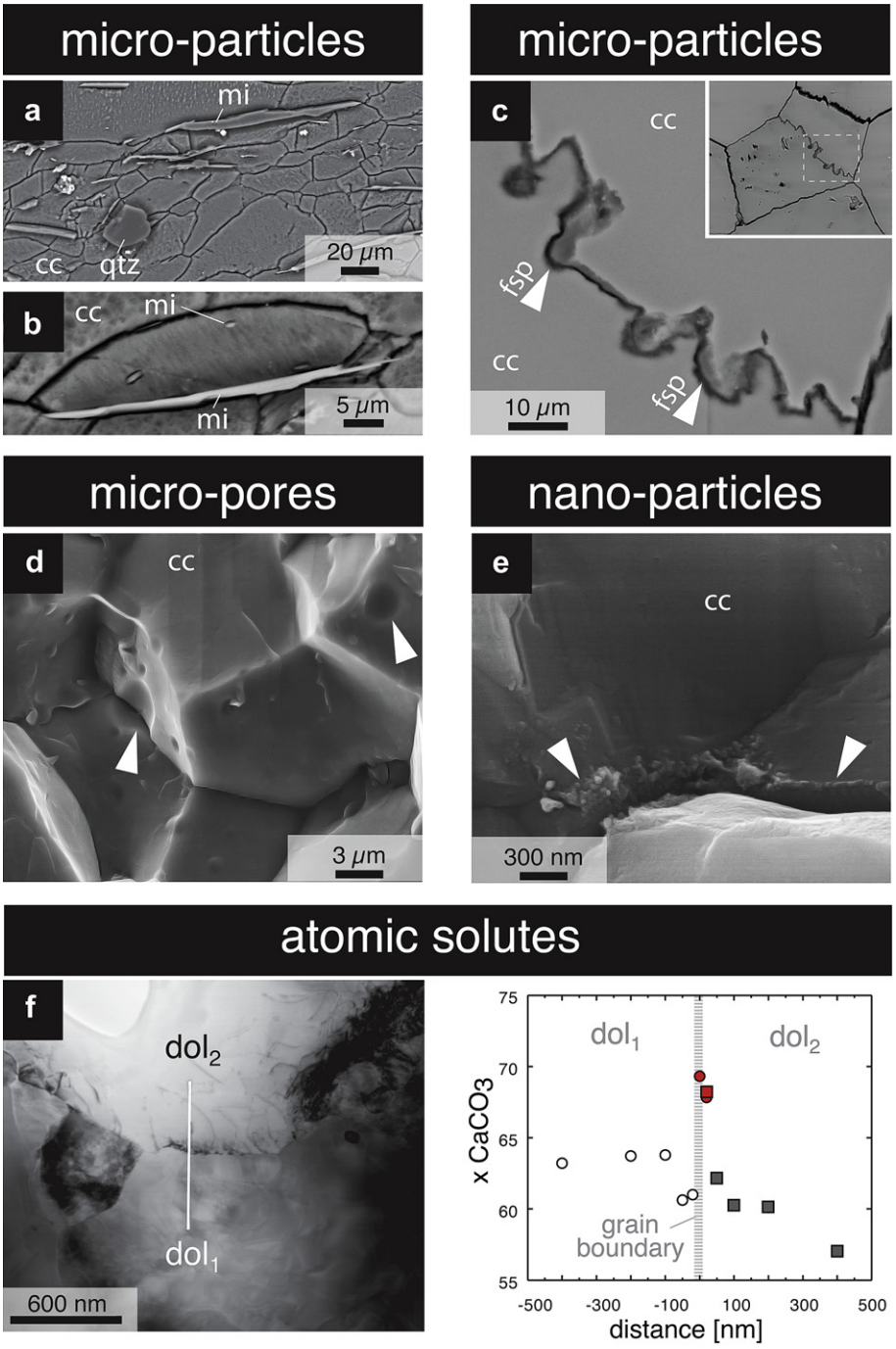

Fig. 1. Effects of second phases on migrating grain boundaries in aggregates with a dominant calcite matrix. (a, b) Calcite grain boundaries of a mylonite from the Doldenhorn nappe (380 °C) pinned by mica as dominant second phase (BE-images). Note the mica grains at grain boundary and included in the calcite grain in (b). (c) Contact metamorphic marble with equilibrated straight calcite grain boundaries (inset) contrast with the lobate grain boundaries resulting from pinning by micrometer-sized feldspar grains (Calcare di Angolo, Adamello contact aureole, 450 °C, BE-image). (d) Pinning of calcite by grain boundary pores during grain growth experiment (hot isostatic pressing, 300 MPa, 850 °C, 2 h; fractured surface, BE-image). (e) Accumulated organic nanoparticles at calcite grain triple junctions inducing dragging forces on the moving calcite grain boundaries (Calcare Dossi dei Morti, Adamello contact aureole, 445 °C; fractured surface, BE-image). (f) Segregation of Ca ions along a dolomite–dolomite grain boundary during grain growth experiment (hot isostatic pressing, 300 MPa, 800 °C, 20 min); TEM image (left) with location of chemical profile, (right) spatial variations in Ca concentration along the profile.

Crump, 1997). Geometrically, an Arrhenius-type law describes this process for normal grain growth (see Evans et al., 2001):

$$\left(D^n - D_0^n\right) = k \cdot \exp(-Q/RT) \cdot \Delta t$$

where D and D_0 are the final and initial grain size, respectively, n is the growth exponent, k a pre-exponential constant, Q the activation energy, R the universal gas constant, T the temperature and Δt the time interval over which grain growth took place (Joesten, 1991). In the case of a polymineralic aggregate, second-phases can either severely slow down the velocities of moving grain boundaries or result in their complete immobilization (Olgaard and Evans, 1986, 1988 and Fig. 6 in Brodhag and Herwegh, 2010; Hiraga et al., 2010). Consequently, smaller grain sizes occur in

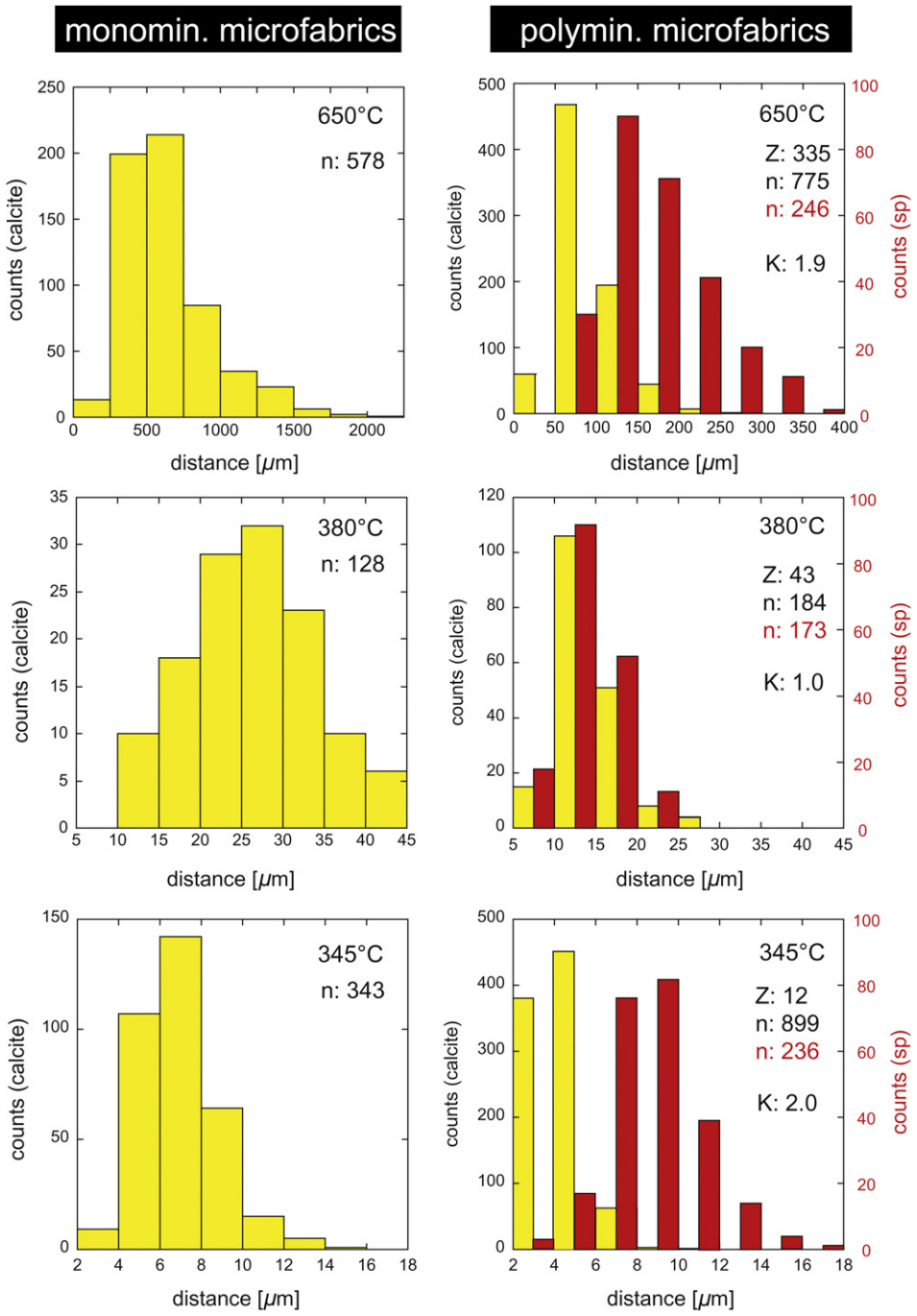

Fig. 2. Diagram shows interparticle distances between grain centers calculated on the base of the five nearest neighbors of each matrix (yellow) and second phase (red) grain (calcite mylonites deformed at different temperatures; 345 & 380 °C Doldenhorn nappe, 650 °C Naxos). Left column: monomineralic fabrics; right column: polymineralic fabrics. Note wider distribution and larger mean value of particle distances for the monomineralic samples, while polymineralic samples display smaller interparticle distances of matrix grains correlating with the smaller spacing of the second phases, the latter controlling the size of the matrix calcite. The K value is defined as the ratio between the mean interparticle distance of the second phases and the one of the matrix grains. If $K > 1$, the matrix grain size is controlled by the second phases (See Brodhag and Herwegh, 2010). Z represents the Zener parameter, i.e., the ratio between the size and volume fraction of the second phases (see text for more details).

polymineralic aggregates compared to monomineralic ones, which coarsened under identical physical conditions (e.g., trend I in Fig. 5). Larger sizes of the individual second phases or clustering of many smaller sized second-phase particles will impose higher drag forces (see Eq. (1)) inhibiting matrix grain growth.

Depending on size and volume fraction of second phases, four major pinning types occur: (i) clustered-particle, (ii) multi-particle and (iii) single-particle pinning, the latter combined with triple junction pinning (Brodhag and Herwegh, 2010; Brodhag et al., 2011; see their Fig. 8 and 9), and (iv) pinning due to crystallographic misfit between adjacent grains (see also Piazolo et al., 2005; Gottstein et al., 2006). Simply based on the second-phase volume fraction and on the spatial arrangement of the individual particles, increasing Z values in Zener space (Fig. 5) are related to a transition from pinning type (i) at low Z, to pinning type (iii) at high Z values, indicating an increase in the

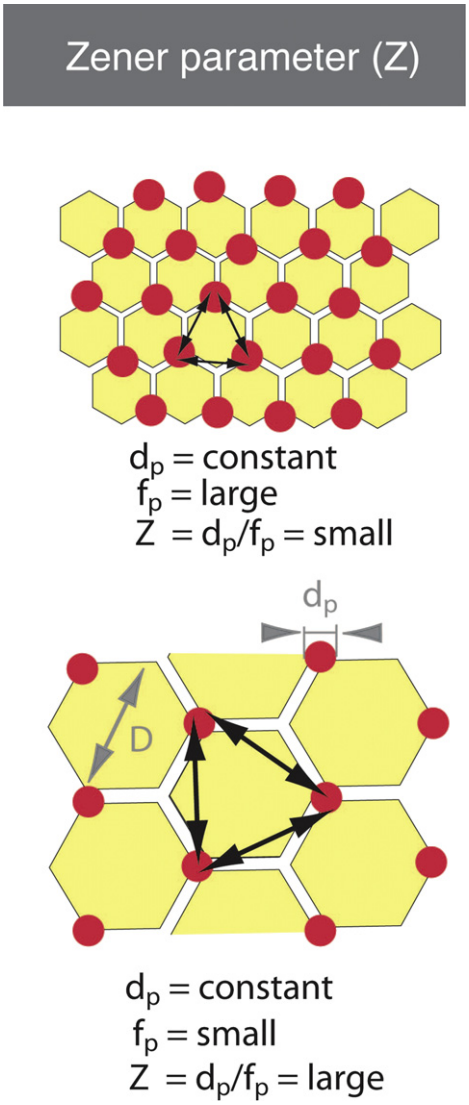

Fig. 3. Effect of the Zener parameter (Z), defined by the ratio between size (d_p) and volume (f_p) fraction of the second phases. Small and large Z typically characterize poly- and nearly monomineralic domains, respectively. Large volume fraction and small sizes of second phases result in a small Z. Small Z means small interparticle distances between second phases, leaving only limited space for the matrix phase to grow and therefore forcing the matrix grain size (D) to stay small. The larger Z becomes, the larger d_p and/or the smaller f_p yielding in larger D.

matrix grain size at given temperature (trend II in Fig. 5a, e, f and examples in Fig. 6).

The geometric relationships between matrix grains and second phases are modified with increasing temperature. The physical reasons for these changes are: (a) the minimization of surface energy and (b) the building up of chemical gradients.

(a) Minimization of surface energy induces the growth of both matrix grains and second phases. This growth requires the operation of three processes: dissolution, mass transfer and precipitation. For the growth of the second phases, all grain boundaries serve as transport pathways for mass exchange between the individual second-phase particles. Amongst the second phases, some will grow while others are completely dissolved (Fig. 5, left column). This overall coarsening of second phases results in a smaller number of grains per unit volume but larger grain sizes, leading to a larger interparticle spacing between second phases. As a consequence, the matrix grains can grow until they are pinned again by the second phases with the new interparticle spacing (see Figs. 3 and 5). The simultaneous growth of both matrix and second-phase grains is referred to as coupled grain coarsening (Alexander et al., 1994; Higgins et al., 1992; Herwegh et al., 2005a; Berger et al., 2010). During coupled grain coarsening, the ratio of matrix- to second-phase grain size remains constant with increasing temperature (see Fig. 7 in Berger et al., 2010). Moreover, small second phases can be integrated into the interior of matrix grains by overgrowth (Berger et al., 2010; Brodhag et al., 2011). In this case, they are no longer part of the bulk chemistry of the grain boundary network. The type and amount of included grains might therefore indirectly affect coupled grain coarsening behavior (see below).

(b) The role of chemical gradients along and across grain boundaries influence coupled grain growth and coarsening. Once a mineral becomes unstable with changing P-T conditions, mineral reactions occur (see Fig. 5 left column, e.g., Carlson and Denison, 1992; Spear, 1993; Carlson and Gordon, 2004; Hirsch and Carlson, 2006). The grain boundary network, which is effectively defined by the size of the matrix grains, controls chemical mass transfer because grain boundaries serve as fast diffusion pathways (Fig. 5a and b; Fig. 6a–c, Farver and Yund, 1996, 1998). Coupled grain growth and nucleation and growth of second phases will change the volume fraction as well as the grain-size distribution of the different second phases, which directly affects the pinning of the matrix grains. Coupled grain coarsening with the new second-phase mineral assemblage controls the microstructure until the next mineral reaction will take place (Fig. 5b–d). For example, several mineral reactions took place in the contact metamorphic aureole of the Adamello pluton (see Berger et al., 2010; Brodhag et al., 2011; Muller et al., 2009) leading to the nucleation of new phases like phlogopite, tremolite or diopside (see Fig. 6a–c).

For both aforementioned behaviors variations in elastic stresses due to direction dependent anisotropic expansion coefficients may additionally promote local dissolution – precipitation along grain interfaces (Brunner, 1984; Frederich and Wong, 1986). More work is required in future with respect to these thermoelastic effects.

At low Z values, a larger volume fraction of second phases is present and pinning keeps the matrix grain size small. In this case, the coarsening of the second phases is rate-limiting for coupled grain coarsening, as it controls the growth of the matrix grain size. We refer to this situation as second-phase controlled coupled grain coarsening (Fig. 5, Brodhag et al., 2011). Note that all microstructures with second-phase volume fractions larger than 0.1 will undergo such second-phase limited grain coarsening (trend I in Figs. 5 and 6), because of the large number of interfaces compared to the reduced number of matrix – matrix grain boundaries (Fig. 7). In contrast to second-phase limited grain coarsening, a small number of second phases located on grain triple junctions control the pinning of the matrix grain size at high Z, where the growth of the second phase particles is of subordinate importance for the overall increase in matrix grain size. This situation is therefore referred to as pinning and matrix controlled coupled grain coarsening (Fig. 5, Brodhag et al., 2011). This coarsening process, characterized by trend II (Fig. 5), mainly occurs in polymineralic aggregates with a subordinate volume fraction of second phases.

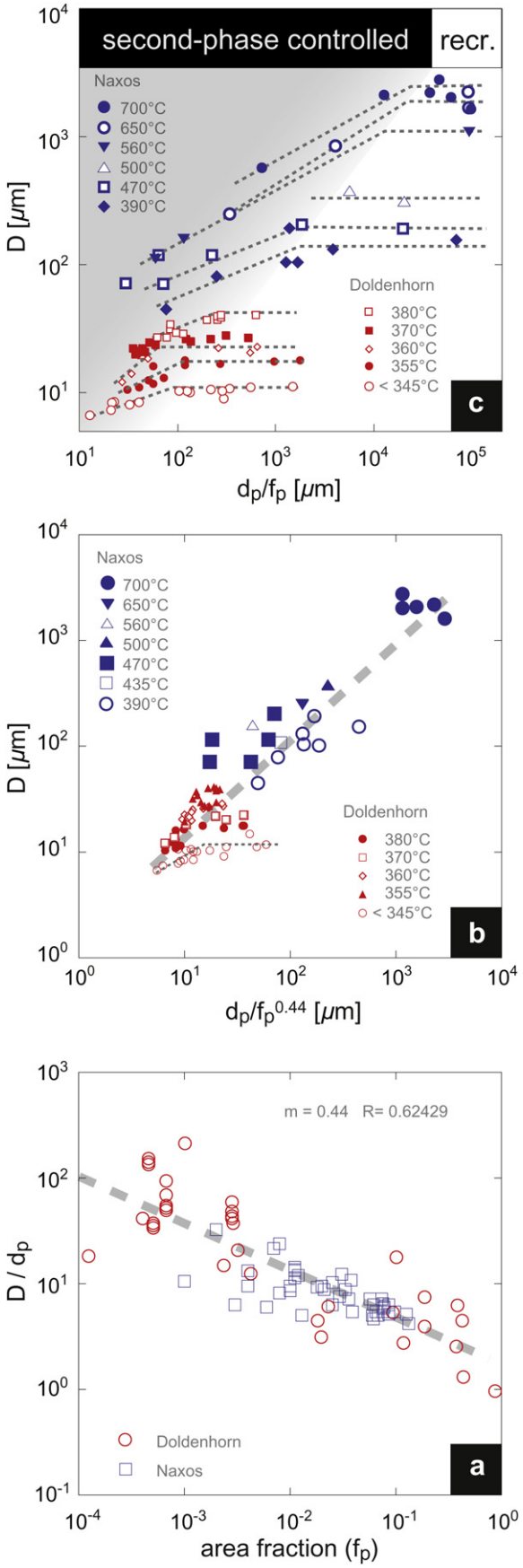

Table 1
m values of Eq. (3) from different polymineralic aggregates.

Polymineralic mixture	Samples	m value	Data reference
Calcite – Al_2O_3	Experiments	0.3–0.55	(Olgaard and Evans, 1986)
Calcite–mica	Experiments	0.3–0.5	(Olgaard and Evans, 1988)
Calcite–mica	Metamorphic	0.36	(Mas and Crowley, 1996)
Calcit–mica	Mylonites	0.24–0.39	(Ebert et al., 2008)
Calcite–mica	Mylonites	0.44	This study (Fig. 4a)
Quartz–graphite	Mylonites	0.4	(Krabbendam et al., 2003)
Gabbro	Mylonite	0.41	(Mehl and Hirth, 2008)
Olivine-enstatite	Experiments	0.59	(Hiraga et al., 2010)
Peridotite	Mylonite	0.35	(Linckens et al., 2011b)

5.2. Grain coarsening processes under regional metamorphic conditions

The knowledge on grain growth and coarsening processes obtained from contact metamorphic marbles (Schmid, 1997; Herwegh and Berger, 2003; Berger and Herwegh, 2004; Berger et al., 2010; Brodhag et al., 2011) can be compared to data from regional metamorphic studies (Fig. 8a and b). Despite longer growth intervals in the latter case, the growth and coarsening processes should be rather similar provided that the effect of deformation is limited. Figure 8b shows data of Mas and Crowley (1996) from a sample suite from the regional metamorphic Shelburne marbles (Berkshire massif). Using the general coarsening trends from the contact metamorphic example of the Adamello pluton (Herwegh and Berger, 2003; Brodhag et al., 2011) and combining them with the regional metamorphic data of Mas and Crowley (1996), yields a good agreement in Zener space (Fig. 8b, see Fig. 13 in Berger and Herwegh, 2004). Hence, we infer that the same coupled grain coarsening and pinning processes occurred in the regional metamorphic samples. Despite the aforementioned differences in time interval, a similar magnitude in grain sizes is obtained for the polymineralic aggregates. This correlation might be attributed to the power-law form of the grain coarsening equations (e.g., see equation (9) in Brodhag and Herwegh, 2010). Very long growth periods would be required to obtain substantial increases in grain size (Herwegh et al., 2005a).

In metamorphic rocks, second-phase controlled coupled grain coarsening compared to pinning and matrix controlled coupled grain coarsening represent two contrasting processes. The latter always results in larger matrix grain sizes. This difference in the growth/pinning behavior in domains with initial compositional variations can result in grain size variations of up to 2–3 orders of magnitude for metamorphic rocks with compositional banding, i.e. with varying REVs for samples with identical P-T evolution (see Figs. 5, 6 and 8). Besides temperature as first order parameter, initial spatial compositional variations in the host rocks can therefore induce considerable microstructural variation during metamorphism. The preservation of such grain size variations during metamorphism is of great importance for any diffusion-controlled process (e.g., the growth of porphyroblasts or the onset of deformation under diffusion creep/granular flow conditions), where

Fig. 4. The Zener space as defined on the base of matrix grain size (D) and the ratio between grain size (d_p) and volume fraction (f_p) of second phases is illustrated with an example (carbonate mylonites form the Doldenhorn nappe (Swiss Helvetic Alps) and Naxos, Greece). (a) The f_p versus D/d_p diagram yields a slope (m) of 0.44 indicative for pinning by second phases at grain boundaries and grain triple junctions (see text). Note considerable data scatter. (b) The d_p/f_p^m versus D diagram shows that isothermal datasets vary in a consistent manner with increasing d_p/f_p^m (see for example 345 °C samples). (c) Using the original d_p/f_p ratio, as defined by Zener in Smith (1948), unravels two microstructural domains, where the calcite grain size either is second-phase (left) or dynamic recrystallization (recr.) controlled (right).

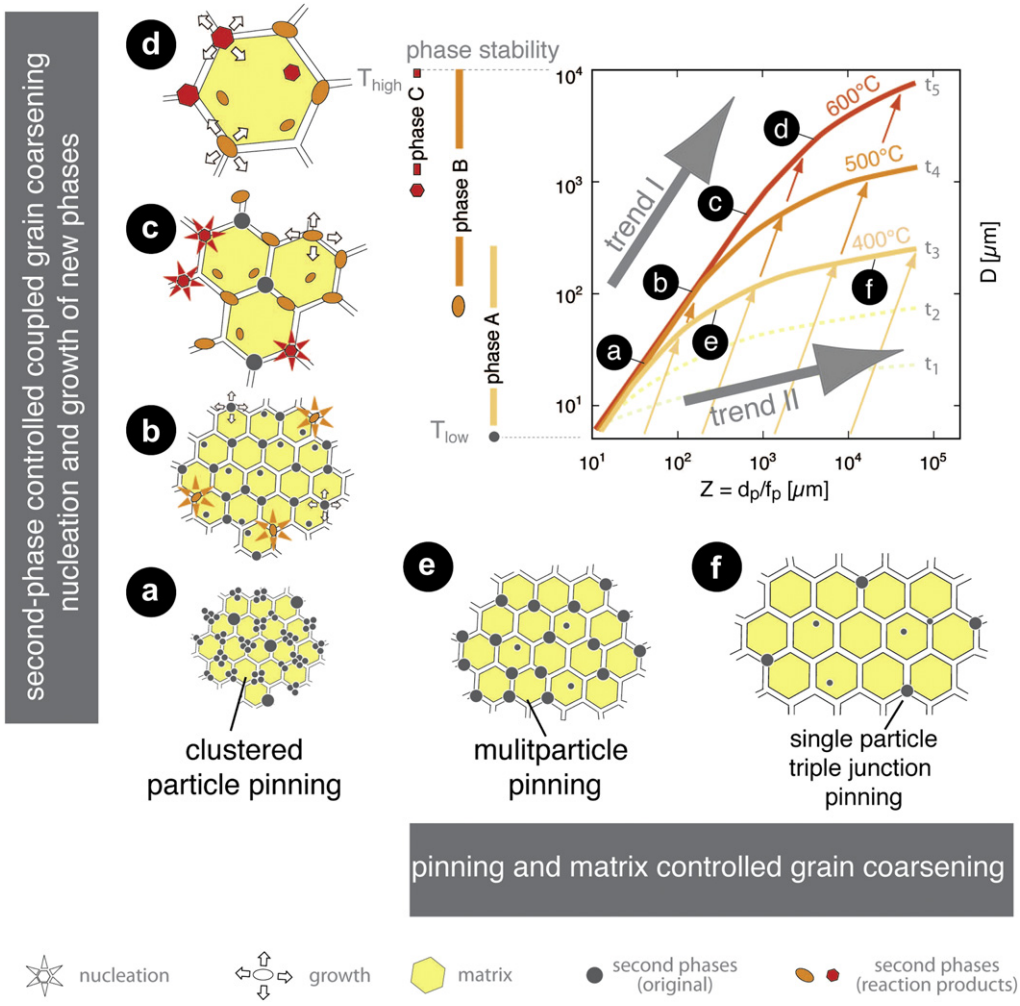

Fig. 5. Schematic illustration showing microstructures in a polymineralic aggregate during grain coarsening under static conditions (based on Brodhag and Herwegh, 2010 and Brodhag et al., 2011): Zener diagram and corresponding microstructures (a–f). Grain growth in a polymineralic system is controlled by the pinning behavior of the second phases (grey, orange and red particles). While at low second-phase volume fraction (f_p; high Z, see f), the boundaries of the matrix are affected by few single particles and triple junctions, multiparticle and clustered particle pinning become the dominant pinning processes with increasing f_p (low Z, see a,e). Two trends result: second-phase controlled coupled grain coarsening (steep trend I, a–d) and (2) matrix controlled (flatter trend II at higher Z; a, e, f) grain coarsening. With increasing T, in addition to the coupled grain coarsening process, also mineral reactions occur involving nucleation and growth of new phases. They will also affect the bulk coarsening behavior of the aggregate (see b–d, and corresponding stability fields of phases A–C). Colored arrows indicate coarsening of both matrix grains and second phases at given volume fractions.

finer grained domains promote diffusion processes due to the large abundance of fast diffusion pathways.

6. Deformation microfabrics

6.1. Dynamic grain size stabilization in monomineralic mylonites

In the second half of the last century, it was first recognized in material sciences and then in rock mechanics that, at high shear strains, rock strength may attain mechanical steady state, i.e. a strain invariant stress state, under certain physical conditions (e.g. Ashby and Verall, 1973; Doherty et al., 1997). In Earth science literature, Etheridge and Wilkie (1979) suggested that mechanical and structural steady state evolve at a rate uniquely defined by the recrystallized grain size (see also piezometric relationship; Twiss, 1977; Vanderwal et al., 1993; Rutter, 1995; Stipp et al., 2010). To achieve a steady-state grain size, (1) grain-size reduction and (2) grain-growth processes have to be balanced over time, in order to obtain a microstructure whose preservation processes are in equilibrium for the given physico-chemical conditions of deformation (Fig. 9). Besides grain size, also other microstructural and textural parameters, like SPO (Means, 1981; Ree, 1991; Herwegh and Handy, 1998) and CPO (Herwegh and Handy, 1996, 1998; Barnhoorn et al., 2004) achieve strain invariant steady state orientations.

(1) Potential grain size reducing processes include subgrain rotation recrystallization (Poirier and Guillopé, 1979; Urai et al., 1986; Drury and Urai, 1990; Shimizu, 1998; Pieri et al., 2001; Barnhoorn et al., 2004), bulging nucleation (Drury and Urai, 1990; Hirth and Tullis, 1992; Stipp et al., 2002a), or the nucleation of new grains either by direct precipitation out of a fluid or by brittle damage and growth of submicroscopic grain fragments (e.g., van Daalen et al., 1999; Vernooij et al., 2006) (Fig. 9a). In natural calcite mylonites, different grain size reducing mechanisms are active at the same time (Herwegh et al., 2005b; see their Fig. 3), but some of the processes can be dominant depending on the physical conditions of deformation (e.g. Hirth and Tullis, 1992; Gleason et al., 1993; Stipp et al., 2002a,b).

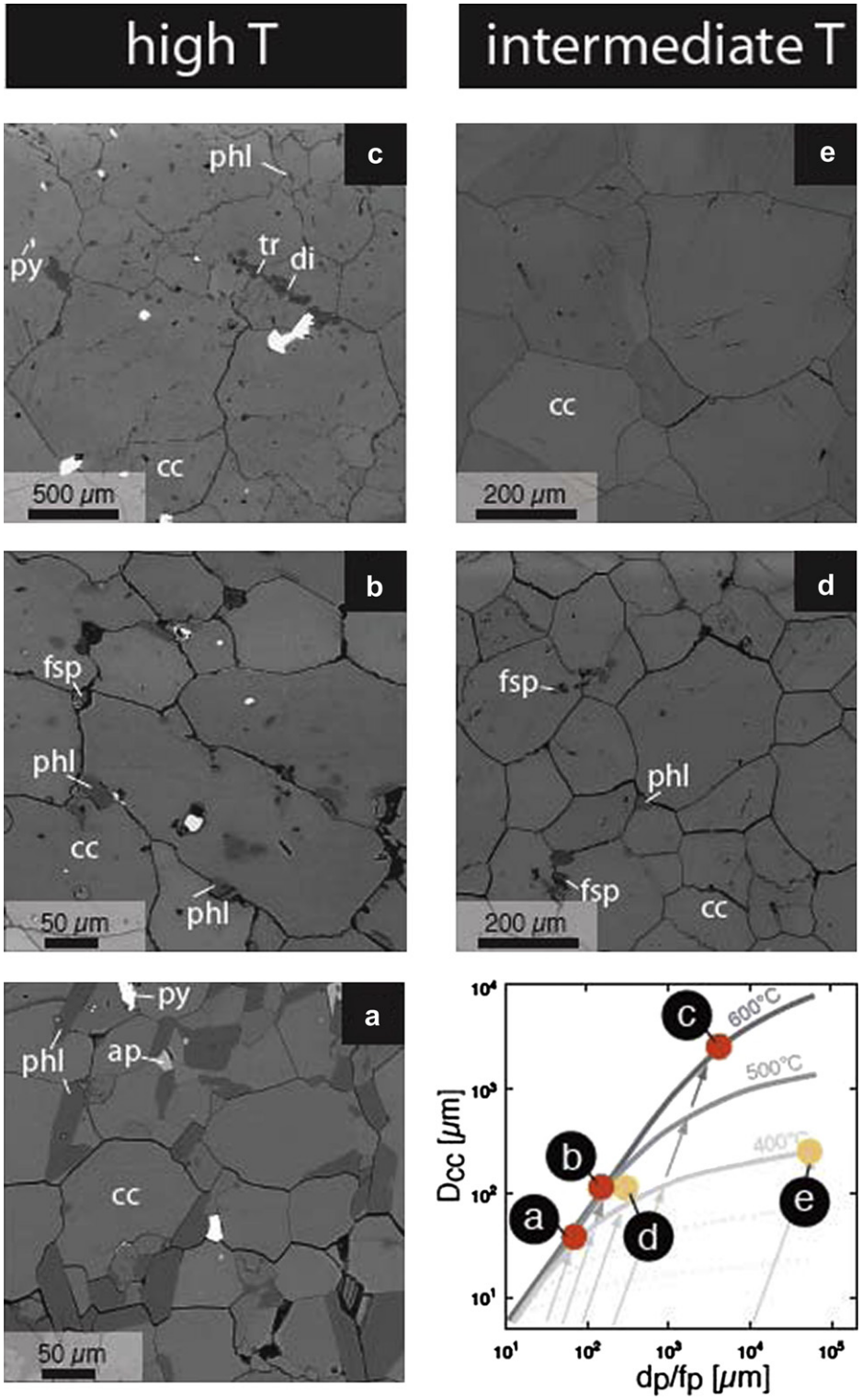

Fig. 6. Microstructural evolution in polymineralic carbonates of the Calcare di Angolo from the Adamello contact metamorphic aureole at high (a–c) and intermediate temperatures (d, e). Locations of the microstructures in the Zener space are indicated in the lower right diagram (larger areas than showed in the micrographs were used for the microstructural quantification). Arrows indicate changes in matrix grain size at constant second-phase volume fractions. High temperature samples: (a) Clustered and multiparticle pinning of matrix calcite (cc) grains by phlogopite (phl) and pyrite (py; T: 595 °C). (b) Multiparticle pinning of calcite by intermediate size phl and feldspar (fsp; T: 630 °C). (c) Multiparticle pinning by tremolite (tr), diopside (di) and pyrite (T: 550 °C). Note the continuous increase in calcite grain size with increasing Z. Intermediate temperature samples show single particle (d, T: 445 °C) and/or triple junction pinning (e; T: 455 °C). The latter sample represents normal grain growth of a nearly monomineralic aggregate.

(2) Minimization of surface energy and internally stored strain energy are the two main driving forces for grain boundary migration promoting the growth of individual grains (Poirier and Guillopé, 1979; Urai et al., 1986; Drury and Urai, 1990).

Recent experiments on very fine-grained calcite aggregates deformed in diffusion creep suggest that the grain growth rate during the evolution toward the steady state grain size is rather similar to the one obtained in static grain growth experiments

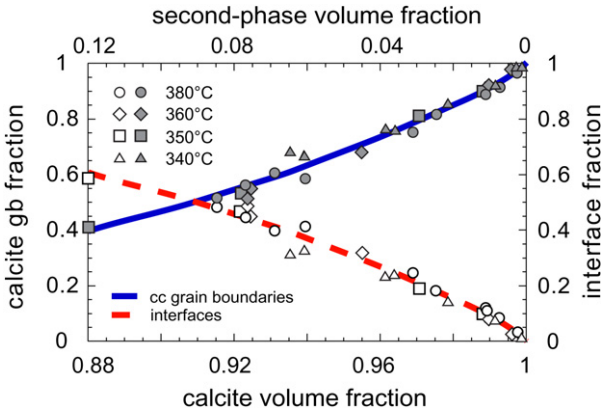

Fig. 7. Changes of calcite grain boundary and interface fractions with increasing second-phase volume fraction (f_p). Note that already a f_p of 0.08–0.1 of second phases reduces the calcite grain surfaces and increases the interfaces to fractions of 0.5. Data derive from polymineralic carbonate mylonites from the Doldenhorn thrust (Helvetic Alps) and are redrawn after Herwegh and Berger (2004).

(Austin and Evans, 2009). Besides grain size also SPO (Means, 1981; Ree, 1991; Herwegh and Handy, 1998) and CPO (Herwegh and Handy, 1996, 1998; Barnhoorn et al., 2004) achieve strain invariant steady state orientations.

In terms of rock mechanics, the piezometric relationship relates differential stress to steady-state dynamically recrystallized grain size (Twiss, 1977) assuming deformation under conditions of dislocation creep. Although being true, it is meanwhile accepted that besides stress, other parameters like strain rate, temperature and chemical gradients like the presence of fluids control the balance between grain size reduction and grain growth. With respect to the latter, de Bresser et al. (1998) introduced the field boundary hypothesis. Here, steady-state grain sizes evolve at the boundary between diffusion creep and dislocation creep (de Bresser et al., 1998, 2001). Based on considerations on the dissipation of energy in the microstructure, more recently, the so-called paleowattmeter was proposed (Austin and Evans, 2007, 2009; Austin et al., 2008; Ricard and Bercovici, 2009). In the case of the paleowattmeter, the energy dissipation required for the grain size reduction in combination with grain growth is used to estimate the contribution of the two processes responsible for the preservation of a steady-state grain size. The common ground of both models is the competition between grain growth and grain size reducing mechanisms, as observed in natural microstructures and rock analog deformation experiments (see Fig. 4 in Herwegh et al., 2005b; Herwegh and Handy, 1996).

6.2. Grain size stabilization in polymineralic mylonites

In contrast to the monomineralic mylonites and the aforementioned stabilization of steady-state grain sizes, in polymineralic mylonites the presence of additional phases controls microstructure and grain boundary mobility of the matrix phase indirectly through pinning. Given the definition of the Zener space, with size (d_p) and volume fraction (f_p) of the second phases controlling the matrix grain size, we will discuss in the following in which manner d_p and f_p can be influenced during the deformation, how second phases recrystallize and what the meaning in terms of their interparticle spacing is.

Drag forces imposed by the second phase interact not only with forces due to grain boundary migration induced by surface energy minimization but also with forces due to thermal-elastic energy (Brunner, 1984; Frederich and Wong, 1986) induced by

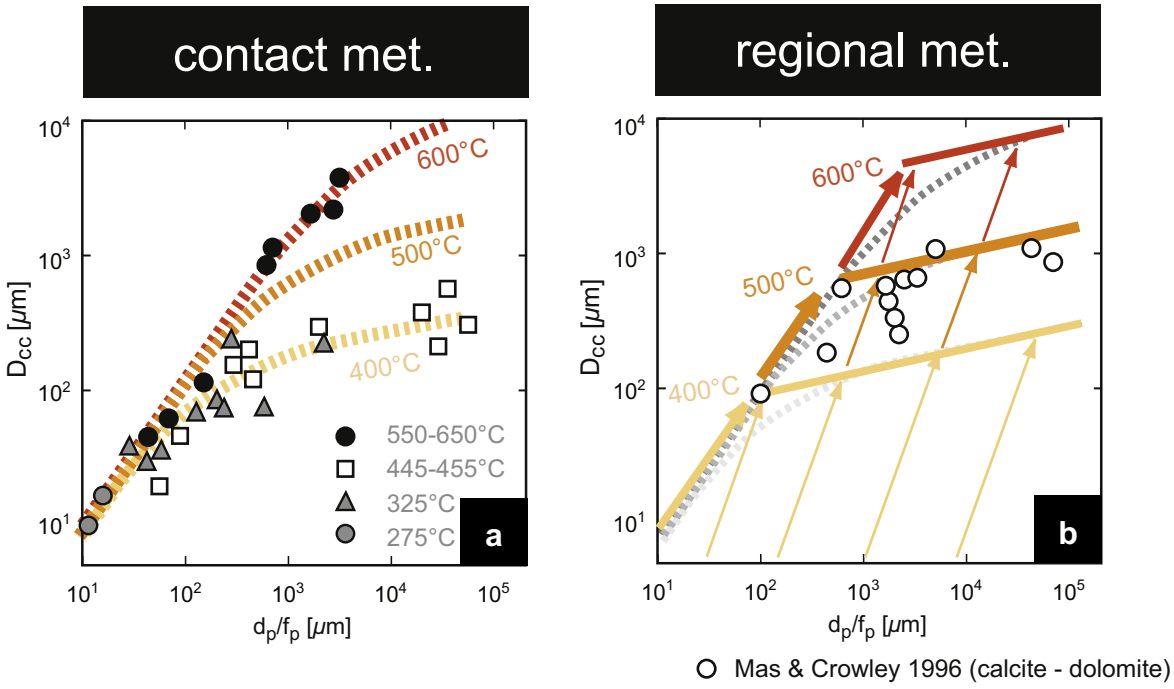

Fig. 8. Comparison between coupled grain coarsening in polymineralic carbonates of the Adamello contact aureole (a, Calcare di Angolo, see Brodhag et al., 2011) and regional metamorphic marbles of the Berkshire massif (b, Shelburne marbles, open circles), which experienced metamorphic temperatures of about 475 °C (Mas and Crowley, 1996). Note the generally larger calcite grain size in the latter owing to the longer growth periods. Nonetheless, the grain sizes fit quite well the temperature range predicted by the contact metamorphic growth. The colored lines in (b) correspond to the generalized growth trends extrapolated from the contact metamorphic situation in (a). Arrows indicate changes in matrix grain size at constant second-phase volume fractions.

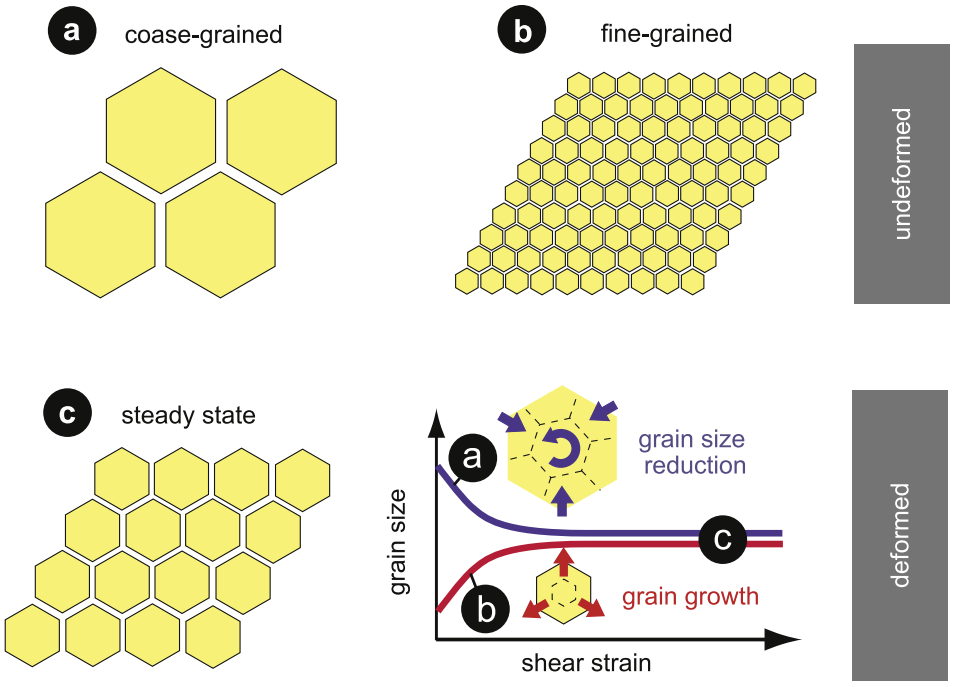

Fig. 9. Schematic presentation of the microstructural evolution on the way to a steady state grain size in a monomineralic mylonite. Depending on a too large (a) or too small (b) starting grain size, grain size reduction or grain growth processes are activated via dynamic recrystallization, respectively, ending in a strain invariant dynamically stabilized steady state grain size (c).

deformation. The size, volume fraction and spatial distribution of the second phases are again the main factors that control the maximum grain size of the matrix phase. Hence, the Zener space can also be applied to describing the microstructural relations between matrix and second phases in deformed polymineralic rocks (Fig. 4c). In analogy to monomineralic rocks, transient stages during the microstructural evolution toward steady state involve grain growth as well as grain size reduction components in polymineralic aggregates (Fig. 10). Grain-scale stress perturbations in the aggregate locally promote dissolution and precipitation facilitating coupled grain coarsening in polymineralic mylonites (Fig. 10a to b). Grain size reduction can take place by dynamic recrystallization, brittle processes or a combination of both (Fig. 10c to b). Which of these processes is activated, depends on the mechanical strength and the deformation mechanisms of each phase at given deformation conditions. Moreover, strain incompatibilities between individual grains can lead to local cavitations or grain boundary voids at grain boundaries (Etheridge and Wilkie, 1979; Ree, 1994; Rybacki et al., 2008; Fusseis et al., 2009). Pore fluid pressures drop due to the local porosity increase and the solute concentration in the fluids are oversaturated leading to precipitation of phases in order to re-establish local chemical equilibrium. This process sequence enables nucleation of new phases (Herwegh and Jenni, 2001; Ebert et al., 2008). These new phases constitute new second-phase grains affecting matrix grain growth as described above (Fig. 10).

Second phases in polymineralic rocks can undergo cycles of nucleation, growth and dissolution similar to individual grains in monomineralic mylonites as indicated by calcite-mica mylonites (Herwegh and Jenni, 2001; see their Fig. 3, 5 and 7). Evidence for such cycles is the preservation of small inclusions in grain interiors (Ebert et al., 2007a). Also the fact that the retrograde overprint of peak metamorphic polymineralic microfabrics results in identical ones as generated on the prograde path under identical deformation conditions supports the idea of a continuous dynamic adaptation by the aforementioned cyclical behavior. Since the exchange of mass between widely spaced second phases is most efficient along grain boundaries, it is again the distribution of both matrix and second phases, which controls the rate of mass transfer processes. One important point with respect to the spatial distribution of second phases is the reduced importance of phase clustering in polymineralic mylonites compared to the static case, implying reduced overall pinning forces due to the sole presence of single phase pinning as weak pinning process. Kruse and Stünitz (1999) referred to this geometrical relationship as anticlustering, where grain boundary sliding and the nucleation of new grains result in homogeneous mixtures of the different phases. Homogenous phase distributions are very common within individual layers of polymineralic tectonites leading to layer-parallel intercalations of microstructural domains with varying second-phase contents (see also Krabbendam et al., 2003; Herwegh and Berger, 2004; Ebert et al., 2007b, Linckens et al., 2011b).

6.3. Deformation mechanisms in polymineralic mylonites

At elevated temperature conditions, monomineralic mylonites preferentially deform under dominance of dislocation creep conditions (e.g., Schmid and Handy, 1991; Kohlstedt et al., 1995). Dynamic recovery in the deforming aggregates is fast enough and associated dynamic recrystallization is capable to achieve grain sizes large enough to prevent significant contribution of diffusion creep (Urai et al., 1986; Drury and Urai, 1990). In contrast, grain sizes of the matrix phase can be kept small in polymineralic mylonites because of the aforementioned pinning processes (Krabbendam et al., 2003; Herwegh and Berger, 2004; Ebert et al., 2008; Linckens et al., 2011b). This pinning and the associated high surface area, promoting diffusional exchange processes, can force the aggregate to deform under diffusion creep. Under circumstances, the presence of second phases can induce a switch

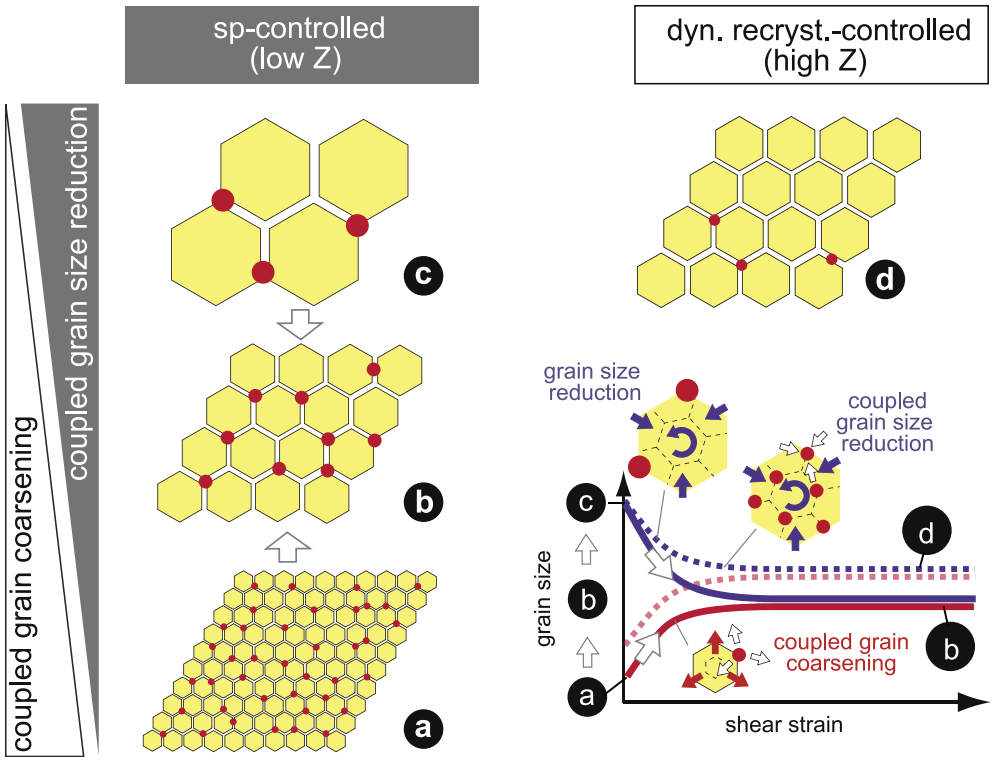

Fig. 10. Schematic illustration of microstructural changes during deformation in a polymineralic mylonite. For high *Z*, i.e. low second-phase volume fractions, the effect of the second phases on the matrix grain size is subordinate and the steady state grain size is controlled by the dynamic recrystallization processes of the matrix phase (see also Fig. 9). In the case of second-phase controlled microfabrics, the interparticle spacing between the second phases defines the maximum grain size of the matrix. A combination of synkinematic coupled grain coarsening or grain size reduction results in a change of second-phase grain size, second-phase dispersion and matrix grain size. In both cases, stabilized grain sizes evolve with strain, which are smaller than those of the monomineralic aggregates. Stippled lines indicate grain size evolution for monomineralic grains from Fig. 9.

in deformation mechanisms between mono- and polymineralic mylonitic layers (e.g. Olgaard, 1990). It is therefore crucial to understand, how interparticle distances of second phases affect the matrix grain size and how they change with varying deformation conditions. At small Zener values, the interparticle distance between the second phases is short and the growth of matrix grains is limited resulting in second-phase controlled aggregates (Herwegh and Berger, 2004). Straight grain boundaries, equidimensional matrix grains and weak CPO often characterize such microfabrics, all pointing to a predominant deformation by granular flow processes (Fig. 11 bottom-left; Olgaard, 1990; Herwegh and Jenni, 2001; Krabbendam et al., 2003). In the context of polymineralic rocks, we favor the term 'diffusion-assisted granular flow' rather than 'diffusion creep' because it is the dissolution, transport and precipitation of mass in a fluid (aqueous, melt), which enables the accommodation of strain incompatibilities via diffusion at grain boundaries during the rotation and sliding of the grains in the aggregates (Paterson, 1995). These processes can act down to very low temperatures and may involve semibrittle and brittle processes (see below).

At low second-phase contents, i.e. high Z values, the interparticle spacing is large and only few matrix grain boundaries are affected by second-phase particles. Hence, the effect of the second phases on the matrix grain size is negligible. We therefore consider these microfabrics as nearly monomineralic system, where the matrix grain size is solely controlled by dynamic recrystallization as shown above. These microfabrics are referred to as dynamic recrystallization controlled (Herwegh and Berger, 2004). Generally, such microfabrics show stronger CPOs compared to the second-phase controlled ones (Fig. 11), pointing to an enhanced dislocation creep component. The weaker CPOs with decreasing temperature suggest an increasing component of granular flow (e.g., Ebert et al., 2007b). The absolute strength in CPO depends on deformation conditions, namely temperature, stress and strain rate, as will be discussed in the next section.

In second-phase controlled calcite mylonites, a rise in temperature promotes grain growth by coupled grain coarsening yielding continuously increasing interparticle spacing of the second phases (see Fig. 2, left column). Consequently, larger mean grain sizes of both matrix and second phases are established (see Fig. 11, left column). For high second-phase volume fractions, the matrix grain boundaries are severely affected by the large number of second-phase particles. Already a second-phase volume fraction of 0.1 is sufficient to occupy already 50% of the total matrix grain boundaries (Fig. 7). Although dislocations can climb and glide easier at elevated temperatures, dynamic recovery processes by grain boundary migration recrystallization are hindered because of pinning of matrix grain boundaries by second phases. Therefore, the microstructure in polymineralic domains has to accommodate deformation by grain boundary sliding and mass transfer processes, forcing the polymineralic aggregate to deform either by viscous granular flow or by a combination of viscous granular flow and dislocation creep, even at elevated temperatures (Fig. 11 left column, see also Herwegh and Berger, 2004; Herwegh and Berger, 2004; Warren and Hirth, 2006; Mehl and Hirth, 2008; Linckens et al., 2011b). Hence, second-phase controlled microfabrics always show weaker CPOs compared to dynamic recrystallization controlled ones (Fig. 11; Herwegh and Berger, 2004).

The same type of microfabric evolution is also found in peridotites. Quantitative microfabric analyses of numerous mantle

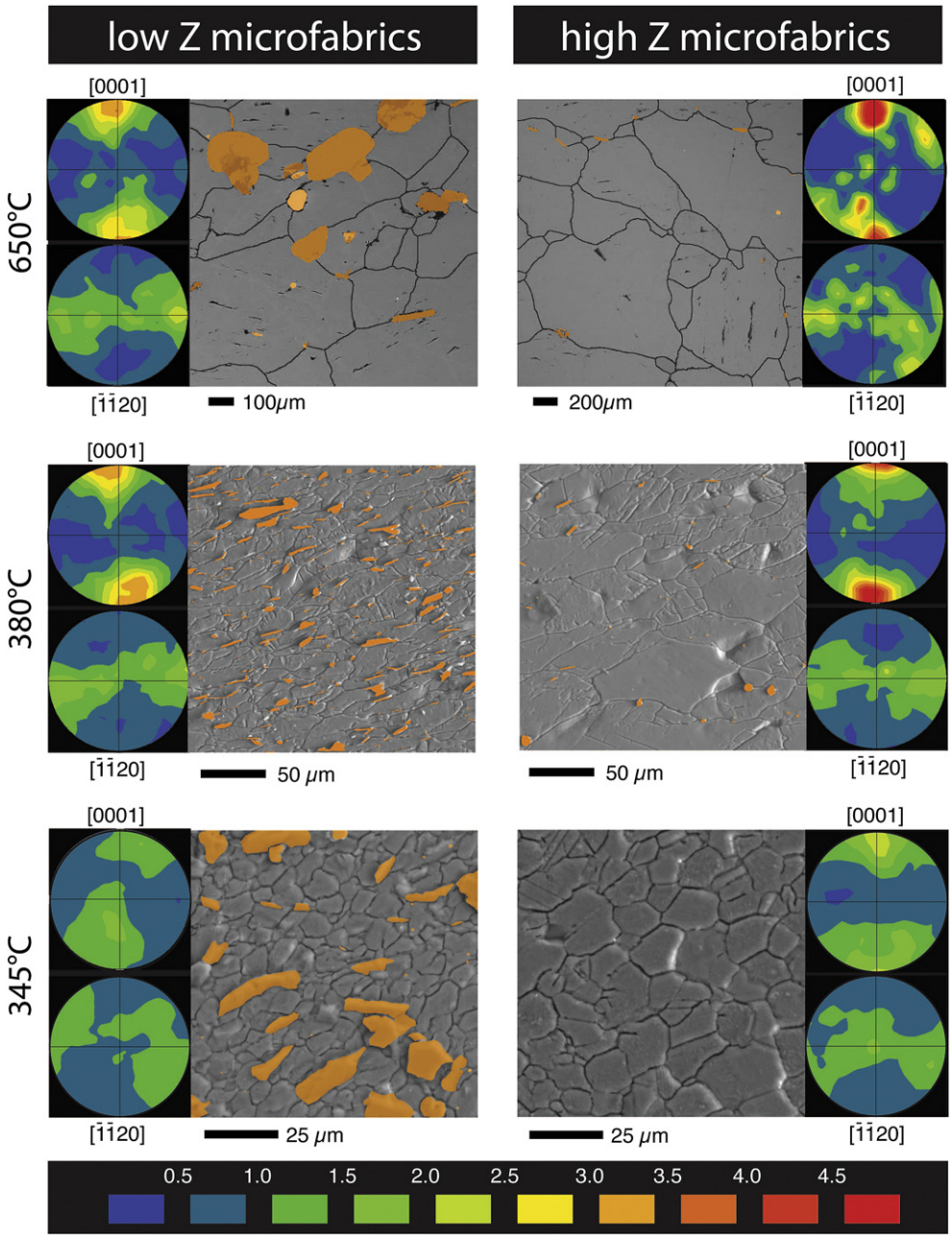

Fig. 11. Compilation of steady state microfabrics from mono- and polymineralic carbonate mylonite layers of the basal thrust of the Doldenhorn nappe (Helvetic Alps, 345 °C and 380 °C) and from Naxos (Greece, 650 °C). At low Z, the calcite grain sizes are always controlled by pinning of the calcite grain boundaries by the second phases (orange, left column), while dynamic recrystallization controls the calcite grain size at high *Z* (right column, see also Fig. 3). The calcite CPO strengths increase both with increasing Z and temperature indicating changes from granular flow dominated to dislocation creep dominated deformation. Bottom row: color code for contour intervals of the stereographic projections of the c- [0001] and a-axes [−1−20].

shear zones deformed in different geodynamic settings (during spreading, in strike-slip zones) suggest that the Zener space describes mantle deformation in general appropriately (Fig. 12, see also Linckens et al., 2011b). Olivine represents the volumetrically dominant matrix phase in these systems, while orthopyroxene (opx), clinopyroxene (cpx), spinel ± plagioclase reflect the second-phase assemblage. Again, recrystallization and second-phase affected microstructures can be discriminated in Zener space (Fig. 12). Grain sizes of matrix and second phases decrease toward lower grade deformation conditions again (Linckens et al., 2011b). Changes in deformation mechanisms are suggested to occur from dominant dislocation creep toward dominant granular flow with decreasing temperature and/or increasing second-phase content (Linckens et al., 2011b). Particularly, recrystallization of the pyroxenes involves a chemical exchange because of disequilibrium and metastability of the pyroxenes with decreasing temperature (Linckens et al., 2011a). In this way, mass transfer combined with dissolution precipitation processes and nucleation of new phases take place. Chemically induced grain boundary migration might contribute to chemical exchange between contacting phases because ions in the solution can directly be incorporated into the lattice of the growing grain (Hillert and Purdy, 1978; Hay and Evans, 1987; Stünitz, 1998; McCaig et al., 2007).

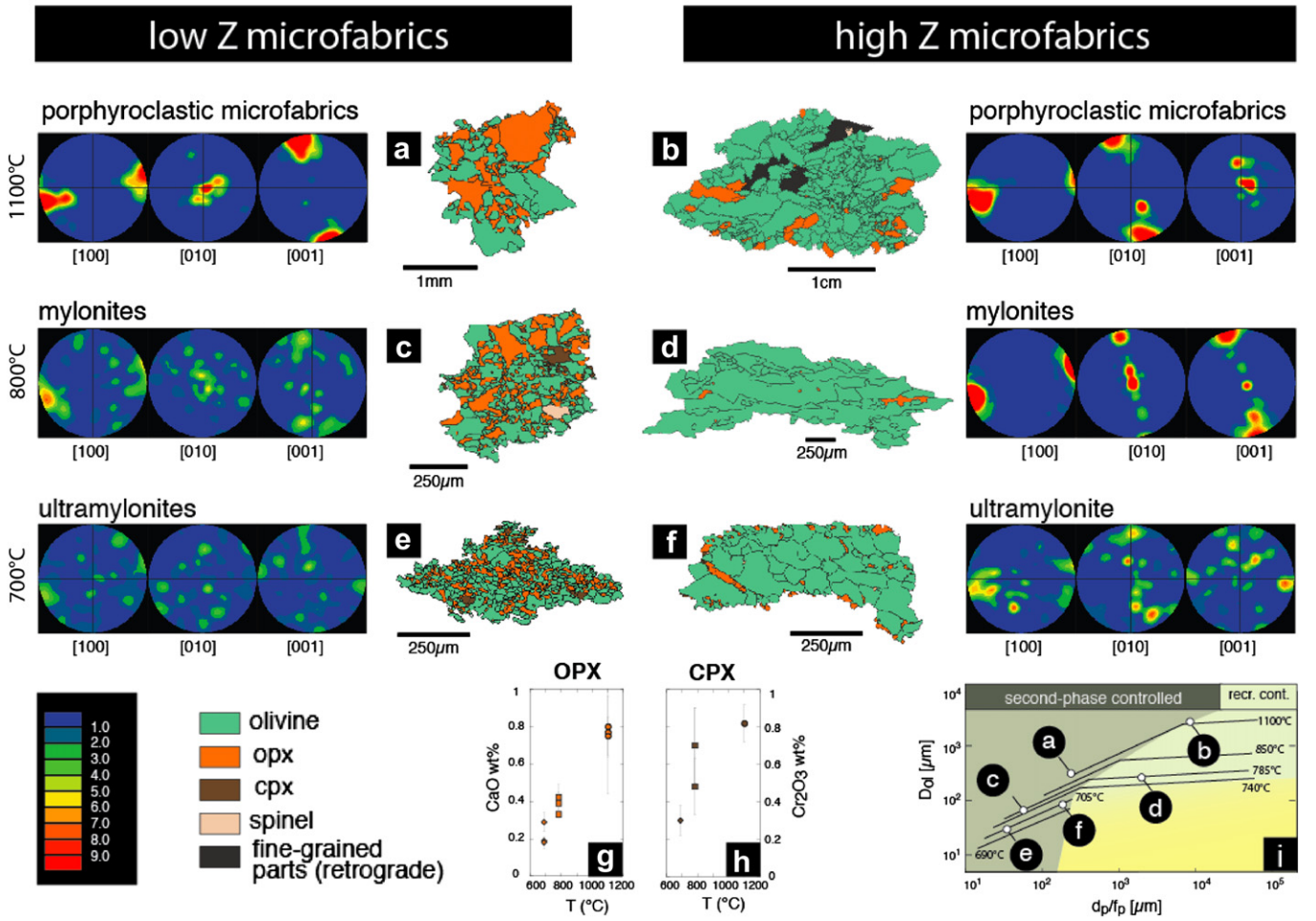

Fig. 12. Evolution of low *Z* and high *Z* microstructures and CPOs in peridotites on the retrograde cooling path (a–f). (g, h) Changes in CaO and Cr_2O_3 content in ortho- (opx) and clinopyroxene (cpx) with temperature indicate a chemical component during recrystallization (data from Linckens, 2010; Linckens et al., 2011b). (i) Location of the microstructural domains (a–f) in the Zener space. Left two legends show contour intervals of the CPOs and color code of the phases in the microstructures. Note strong pinning effect of the olivine grain size by the second phases at low *Z* fabrics, while the grain sizes are much larger in the high *Z* fabrics. CPOs generally are weaker in low *Z* domains and are weakest in the ultramylonites indicating diffusion creep dominated deformation at low temperature deformation. CPO strength increases with temperature in both low and high *Z* microstructures suggesting an increasing dislocation creep component.

The transition from second-phase to dynamic-recrystallization controlled microfabrics seems to be rather common for many different polymineralic mylonites in nature. Fig. 13 displays a compilation of microstructural data from literature for calcite-mica (this study, Fig. 4c), quartz-graphite (Krabbendam et al., 2003), quartz-mica (Song and Ree, 2007), gabbro (Mehl and Hirth, 2008), and peridotite mylonites (Linckens et al., 2011b). All polymineralic aggregates show a systematic discrimination between second-phase and dynamic-recrystallization controlled trends at given temperature (Fig. 13). The positions in Zener space where the transition between the two microstructural trends occurs, however, vary as a function of the mineral systems but also of the deformation conditions. For calcite-mica mylonites from the Helvetic Alps, the transition manifests at second-phase volume fractions of about 0.02–0.03 (Ebert et al., 2008). Owing to the increase in grain size with increasing temperature, however, the Z parameter representing the transition increases as well because of the coarsening of the second phases. This behavior typically yields a steeply inclined boundary between second-phase and dynamic-recrystallization controlled fields in the Zener diagram (see Figs. 12–14). Although a lack of complete datasets prevents a full exploration of Zener space over the entire temperature range for the different mineral systems, we conclude that steady-state matrix grain sizes at a given temperature must vary with second-phase content for different mineral systems. The reason for these variations is attributed to the different kinetics of growth, recovery and mass transfer processes of the systems in general and those of the associated minerals in particular.

6.4. Parameterization of microstructural changes in polymineralic mylonites

The aforementioned datasets can be used to construct so-called grain coarsening or grain-size evolution maps. For calibration of such maps, quantitative microstructural estimates on relations between matrix grain size (D^{poly}_{matrix}) as well as second-phase volume fraction (f_p) and second-phase grain size (d_p) at specific deformation temperatures are necessary. These data are used in a first step to solve for the activation energy (Q^{poly}_{matrix}) related to microstructural changes in the matrix phase. For this purpose, Eq. (4) can be expanded to an Arrhenius-type equation by adding the activation term Q^{poly}_{matrix} (see Berger and Herwegh, 2004; Herwegh et al., 2005a):

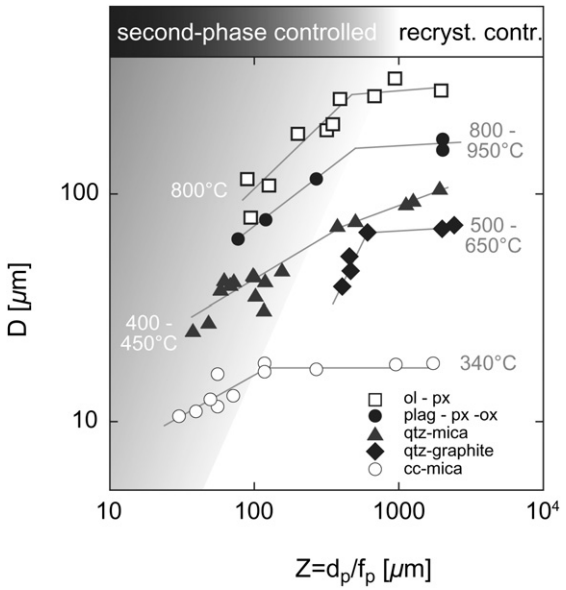

Fig. 13. Zener diagram for different polymineralic rocks all showing a transition from second-phase to dynamic recrystallization controlled microstructures. Olivine - pyroxene (ol-px) peridotite mylonite from Linckens (2010, 800 °C); plagioclase-pyroxene-oxide (plag-px-ox): gabbro mylonites from Mehl and Hirth (2008, 800–950 °C); quartz-mica (qtz-mica): mylonite from Song and Ree (2007, 400–450 °C); quartz-graphite (qtz-graphite) mylonite from Krabbendam et al. (2003, 500–650 °C); calcite-mica (cc-mica) mylonite from Herwegh and Berger (2004, 340 °C). *D*: matrix grain size; *Z*: Zener parameter.

$$D^{poly}_{matrix} = c' \cdot \exp\left(\frac{-Q^{poly}_{matrix}}{RT}\right) \cdot \left(\frac{d_p}{f_p}\right)^{m^*} \quad (6)$$

where c' [μm] is a constant, R [J/mol K] is the universal gas constant, T is the estimated deformation temperature [K], and m^* is the slope of the curve in the Zener diagram (see Fig. 4c). Second-phase grain size also satisfies an Arrhenius-type equation as function of second-phase volume fraction and temperature:

$$d_p = k' \cdot \exp\left(\frac{-Q_p}{RT}\right) \cdot f_p^n \quad (7)$$

where k' [μm] is a constant, Q_p is the activation energy related to grain size changes of the second phases and n is a grain growth exponent (usually 2 or 3, see for example Evans et al., 2001). Q^{poly}_{matrix} and Q_p can be obtained from the slopes of linear best fits to D versus $1/T$ and in d_p versus $1/T$ diagrams, respectively. The constants c' and k' can then be calculated from the equations (for more details consult Herwegh et al., 2005a; Ebert et al., 2008).

Finally, Eq. (7) can be substituted in Eq. (6) yielding:

$$D^{poly}_{matrix} = c' \cdot k' m^* \cdot \exp\left(\frac{-Q^{poly}_{matrix}}{RT}\right) \cdot \left[\exp\left(\frac{-Q_p}{RT}\right)\right]^{m^*} \cdot f_p^{m^*(n-1)} \quad (8)$$

Eqs. (7) and (8) allow the calculations of the changes in matrix and second-phase grain size for different second-phase volume fractions and deformation temperatures. Based on the variation of the latter, the second-phase controlled field of the grain size evolution maps can be constructed.

Eq. (8) can also be employed for mapping the dynamic recrystallization controlled field. If there is no dependence of matrix grain size on second-phase content, represented by a horizontal trend line in Zener space (e.g., polymineralic carbonate mylonites of Fig. 4c), Eq. (8) reduces to:

$$D^{mono}_{matrix} = c'' \cdot \exp\left(\frac{-Q^{mono}_{matrix}}{RT}\right) \quad (9)$$

In this equation c'' [μm] represents a constant while D^{mono}_{matrix} and Q^{mono}_{matrix} are the dynamically balanced matrix grain size and the activation energy, respectively, of the processes incorporated. In the case that there still remains a slight dependence of the matrix grain size on the second-phase content (e.g., peridotites in Figs. 12), Eq. (9) needs to be modified by incorporating a dependence on the Zener ratio (see Eq. (4)):

$$D^{mono}_{matrix} = c''' \cdot \exp\left(\frac{-Q^{mono}_{matrix}}{RT}\right) \cdot \left(\frac{d_p}{f_p}\right)^{m^*_{mono}} \quad (10)$$

Grain size evolution maps have been calibrated for polymineralic carbonate mylonites (Herwegh et al., 2005a; Ebert et al., 2008, see Table 2) and peridotite mylonites (Fig. 14; see also Linckens, 2010). Such maps are useful for the following reasons: (i) Microstructural data (D^{mono}_{matrix}, f_p, d_p) from natural shear zones can be used to estimate the deformation temperature; (ii) predictions of the variations of matrix grain size with varying f_p and d_p can be made for a given deformation temperature; and (iii) predictions of the microstructural evolution of polymineralic mylonites can be made for complex temperature histories. The latter will be crucial for numerical and rheological modeling of the geodynamic evolution of large-scale shear zones, especially in cases where strain weakening involves grain-size sensitive deformation mechanisms like diffusion creep.

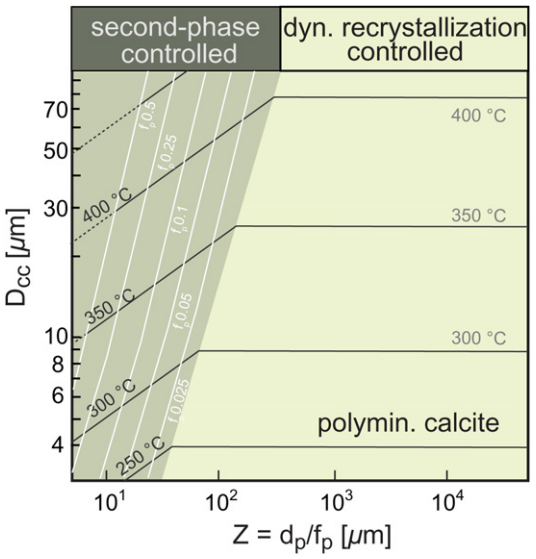

Fig. 14. Grain size evolution maps of polymineralic calcite mylonites. Based on the grain size trends of Zener diagrams like in Fig. 4, empirical grain size evolution maps can be calculated allowing to predict the grain size changes of both matrix and second phases in a polymineralic mylonite as a function of changing T or second-phase volume fraction (f_p). See equations in text and Table 2.

7. Mineral reactions and their effect on polymineralic microfabrics

So far, the polymineralic microfabrics treated were all considered as stable mineral assemblages. Similar to the static example of the contact metamorphic aureole of the Adamello pluton, however,

Table 2
Parameters required for Eq. (8) to construct a grain size evolution map, calibrated on the base of natural calcite mylonites (Ebert et al., 2008). For abbreviations see text.

Parameters (see eq. (8))	Second-phase controlled $T < 350$ °C	Second-phase controlled $T > 350$ °C	Dynamic recrystallization controlled $T < 350$ °C	Dynamic recrystallization controlled $T > 350$ °C	Units
Q_{cc}	32	60	40	80	kJ mol^{-1}
Q_p	40 ± 7	40 ± 7	40 ± 7	40 ± 7	kJ mol^{-1}
n	0.1 ± 0.05	0.15 ± 0.05	0.15 ± 0.05	0.15 ± 0.05	
m^*	0.30 ± 0.05	0.30 ± 0.05	0.30 ± 0.05	0.30 ± 0.05	
c'	2.04E + 3	6.22E + 5	3.90E + 4	1.25E+8	μm
k'	8.59E + 3	8.59E + 3	8.59E + 3	8.59E+3	μm

mineral stabilities change during deformation at varying P-T conditions. As a consequence, chemical concentration gradients evolve and mineral reactions occur inducing changes in volume fractions, grain sizes and spatial distribution of phases (e.g., Kruse and Stünitz, 1999; Kenkmann and Dresen, 2002). Such reaction-induced changes will not only influence the location of the microstructures in Zener space but may also dramatically affect the bulk rheology of the polymineralic rocks. Nucleation of new mechanically weaker phases, release of water due to dehydration reactions, hydrolitic weakening because of incorporation of water into the lattice or stress perturbation induced by volume changes are just few effects to be named in this sense (e.g., Rutter and Brodie, 1988; Stünitz and Tullis, 2001; de Ronde et al., 2005).

At the present stage, no comprehensive studies exist that deal with the effect of synkinematic mineral reactions on phase and grain size distributions in the light of Zener space. We therefore can only speculate on this topic by combining our observations of stable mineral assemblages with data from natural and experimental microfabrics involving mineral reactions. Various experiments were performed to investigate the effect of synkinematic mineral reactions on rock bulk strength (e.g., Stünitz and Tullis, 2001; de Ronde et al., 2005; Holyoke and Tullis, 2006b). As summarized by de Ronde et al. (2005): (i) reactions can produce new small grains that deform by diffusion-accommodated grain boundary sliding; (ii) dehydration may lead to weakening of the aggregates due to increased pore fluid pressures, (iii) solid state deformation may cause weakening by transformation plasticity or (iv) reactions may result in new phases with lower rock strength. In addition, latent heat release during the reaction and the mechanical effect of volume changes inducing stress perturbations have to be taken into consideration. Comparing these different weakening processes, only the formation of new phases will have a long lasting influence on polymineralic mylonites. Examples for the evolution of weak phases during metamorphic reactions are the serpentinization of peridotites (Escartin et al., 2001) or the formation of sheet silicates (Fitz Gerald and Stunitz, 1993; Wintsch et al., 1995; Holyoke and Tullis, 2006a; O'Hara, 2007). The rheological effect of weakening by (i–iii) is in most cases of transient character and the question arises of its durability.

Although many recent experiments convincingly reveal reaction-induced grain size reductions down to the micro-scale (e.g. Stünitz and Tullis, 2001; de Ronde et al., 2005; Holyoke and Tullis, 2006a), the relevance and efficiency of switching from dislocation-creep to diffusion-creep dominated deformation is debatable for different polymineralic natural systems at elevated temperatures. The extrapolation of experimental results assumes that fine-grained aggregates are preserved readily. In contrast to nature, temperature variations in laboratory experiments occur quite quickly provoking a rapid adaptation of the mineral assemblages to the new chemical equilibrium conditions. As a consequence, large amounts of very fine-grained reaction products appear in a short time. In large-scale shear zones, however, such temperature changes proceed at much lower rates. In combination with ongoing deformation, the products of mineral reactions will therefore appear in a more continuous rather than abrupt manner resulting in a progressive change of the rock's modal composition. Because of this reduced grain production rate, newly grown minerals have time to interact with the surrounding matrix minerals allowing for coupled-grain coarsening as presented above in the case of stable mineral assemblages. In fact, coupled grain coarsening would even be promoted in the presence of fluids because of enhanced mass transfer kinetics resulting in faster growth of mineral grains (e.g., see Mancktelow and Pennacchioni, 2004). Therefore, the small recrystallized grains of the reaction products might not be preserved. Hence, the suggested switch from dislocation-creep to diffusion-creep accommodated grain boundary sliding would be of transient character only at elevated temperatures.

However, this rapid switch of deformation mechanisms likely matters during mineral reactions that occur on retrograde metamorphic temperature paths, where no substantial coupled grain coarsening is possible. At low temperature conditions, growth kinetics is so slow that the fine-grained reaction products can be preserved. In such cases, a switch to diffusion-accommodated grain boundary sliding or semibrittle deformation may occur and lead to strain weakening (e.g., Stünitz and Fitz Gerald, 1993, see also peridotites above).

8. Rheology of mono- and polymineralic domains

Profound knowledge of the rheology of polymineralic rocks is crucial, given the fact that most rocks in the Earth's crust and mantle have polymineralic modal compositions. Many experimental studies (e.g., Jordan, 1987; Dresen and Evans, 1993; Dresen et al., 1998; Bruhn et al., 1999; Ji et al., 2001; Rybacki et al., 2003; Xiao and Evans, 2003; Barnhoorn et al., 2005b; Dimanov and Dresen, 2005; Renner et al., 2007; Delle Piane et al., 2009) and theoretical investigations (Tullis et al., 1991; Handy, 1990, 1992; Ji et al., 2003) were carried out to predict the rheology of polymineralic aggregates. Of special interest in terms of strain localization processes is the pinning of grain boundaries by second phases (e.g., Olgaard, 1990; Drury and Urai, 1990). As demonstrated above, pinning processes keep the matrix grain size small and can therefore force the matrix grains to deform by grain-size sensitive deformation mechanisms (diffusion creep, viscous granular flow), with reduced differential stresses in comparison to equivalent dislocation creep. This difference in flow strength is suggested as important factor for strain localization in polymineralic domains (e.g., Olgaard, 1990; Jaroslow et al., 1996; Newman et al., 1999; Toy et al., 2009; Skemer et al., 2010). In nature, polymineralic mylonites often appear as parallel layers, where the layers are characterized by different second-phase contents (Herwegh et al., 2008; Mehl and Hirth, 2008). The observation that mono- as well as polymineralic layers are intercalated and parallel to each other without folds or boudins implies that the layers are nearly equiviscous. Therefore, grain sizes, phase distributions (Herwegh and Jenni,

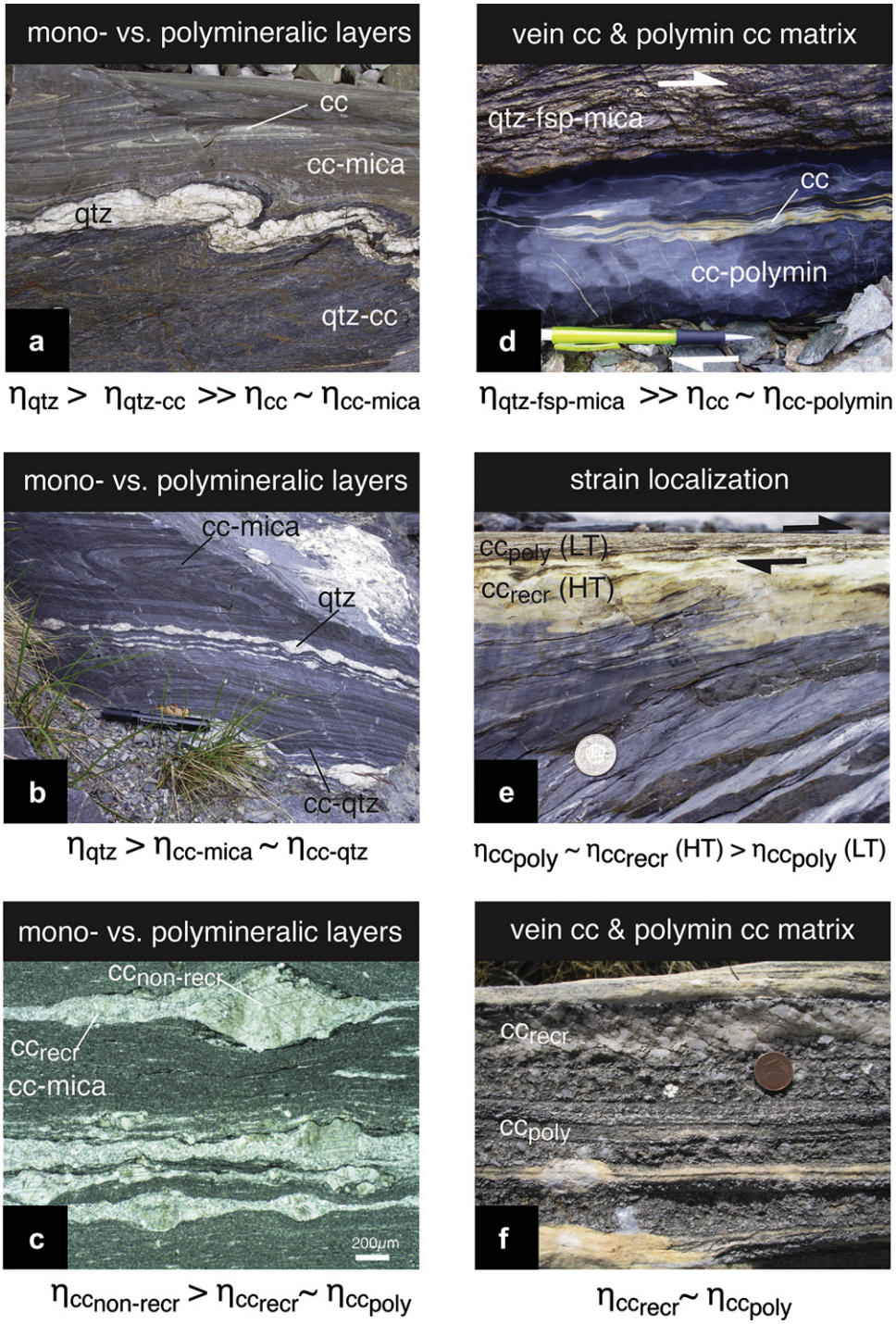

Fig. 15. Deformation structures of mono- and polymineralic carbonate mylonites and inferred relative differences in viscosities (η). (a) Open low amplitude folds of the quartz layer indicate higher viscosity compared to polymineralic qtz-cc layer and the isoclinally folded intercalations of cc-mica and cc-layers (Gault, Morcles nappe, Swiss Helvetic Alps). (b) Parallel cc-qtz-mica intercalations with variations in modal composition point toward similar viscosities, whereas the boudinaged quartz vein indicates a higher viscosity (Gault, Morcles nappe). (c) Micrograph of a boudinaged calcite vein implies higher strength of coarse-grained vein calcite in comparison to the fine-grained recrystallized vein calcite and the polymineralic calcite-mica matrix (Quinten limestone, Doldenhorn thrust). (d) Mechanically strong quartz-feldspar-mica aggregates thrusted on the Lochsiten tectonite consisting at this locality of parallel bands of recrystallized vein calcite and polymineralic calcite layers pointing to a equiviscous flow behavior of the carbonates (Quinten limestone, Glarus thrust). (e) High temperature (HT) mylonites consisting of calcite veins and polymineralic Quinten limestone are folded and sheared into a mechanically weak polymineralic shear zone that evolved under low temperature (LT) conditions. (f) Parallel layers of mono- and polymineralic microstructures of carbonate mylonites suggest similar viscosity (Naxos, Greece). Deformation took place at temperatures between 340 and 550 °C, except in (d) where a low temperature (LT) overprint took place. Cc: calcite; qtz: quartz; fsp: feldspar; cc_{poly}: polymineralic calcite matrix, cc_{recr} and $cc_{non\text{-}rec}$: dynamically recrystallized and non-recrystallized calcite, respectively.

2001; Herwegh and Berger, 2004; Ebert et al., 2008; Linckens et al., 2011b), and associated deformation mechanisms probably self-organize to produce homogeneous deformation by adjusting the contribution of grain-size sensitive and insensitive deformation mechanisms (see discussion above). We thus suggest that for a given deformation temperature under steady state conditions, all microfabrics on the same trend line in Zener space deform under similar flow stresses and strain rates, i.e. show similar effective-

viscosity ratios. As will be elucidated in the following, it follows that strain localization in polymineralic layers is restricted to transient deformation stages, as observed in polymineralic calcite and peridotite mylonites (Figs. 15 and 16).

The effective viscosity of polymineralic calcite-mica layers (Fig. 15) is smaller than that of monomineralic quartz layers at about 330 °C. This is inferred from the reduced wavelength and amplitude of the folds in the quartz band in comparison to those in the calcite-mica layers (Fig. 15a, see also Biot, 1961). Boudinage of coarse-grained and partly dynamically recrystallized monomineralic quartz veins also suggests higher viscosity compared to the polymineralic calcite-mica layers (Fig. 15b and c). Similar observations pertain to the peridotite mylonites in deformation behavior of pyroxene and olivine (Linckens et al., 2011b). Boudinaged coarse-grained pyroxenite layers point toward higher viscosity compared to polymineralic harzburgitic mylonites

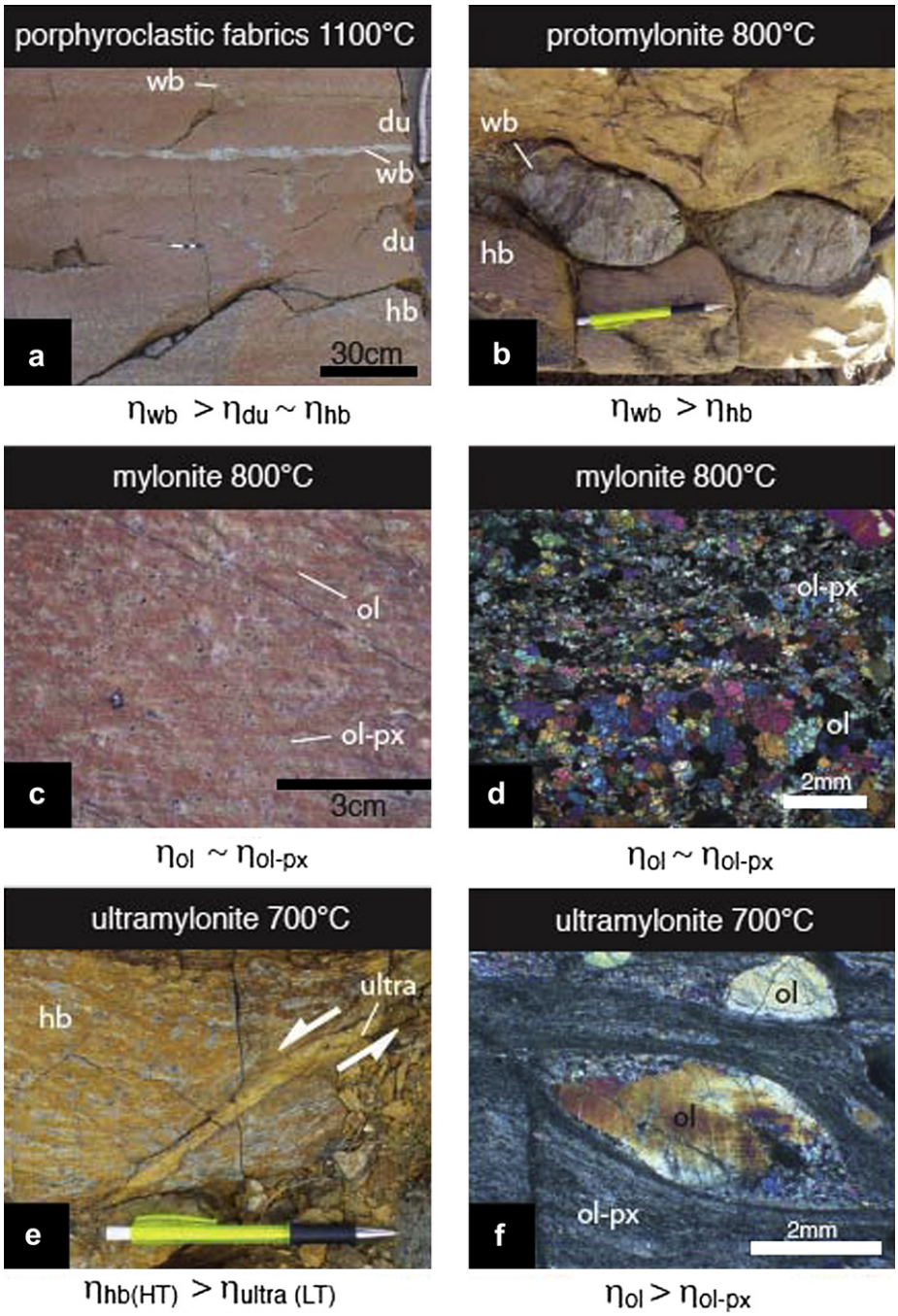

Fig. 16. Deformation structures of peridotites and inferred relative viscosities. (a) Porphyroclastic fabrics with original dunite(du)-harzburgite(hb) layering. Parallel layering of mono- and polymineralic layers suggests deformation under equiviscous conditions at 1100 °C, while boudinage of the websterite dikes (wb) clearly point to higher flow viscosity of the pyroxenes (Wadi al Wasit, Oman). (b) During mylonitic deformation at 800 °C, boudinage of the former websterite dike indicates that pyroxenes are stronger under these conditions compared to the polymineralic harzburgites (Wadi al Wasit, Oman). (c) Strong elongation and parallel layering of olivine (ol) and former pyroxene clasts (ol-px); (d) now existing in form of coarse-grained monomineralic olivine and fine-grained polymineralic ol-px mixtures (scale bar 2 mm, thin section under crossed nicols; Lanzo, Italy), reflect similar viscosity during mylonitic deformation at 800 °C. (e) Strong strain localization in a narrow sinistral ultramylonitic shear zone under low temperatures of 700 °C results in (f) lense-shaped olivine clasts embedded in a mechanically weaker polymineralic fine-grained matrix (scale bar 2 mm, thin section under crossed nicols; Lanzo, Italy).

deformed at about 1100 °C (Fig. 16a,b and Fig. 17). According to the model of Handy (1990, 1992), interconnected mechanically weak phases define the bulk strength of two-phase materials at volume fractions of 0.1–0.2. In our peridotite, the mechanically weak olivine (volume fraction > 0.6) forms an interconnected network. Therefore, the bulk rheology of peridotite will be close to that of olivine (Fig. 17; see also Handy, 1990, 1992, 1994) while the pyroxenes form rigid inclusions and are therefore mechanically stronger (Fig. 16a). In contrast, layers of polymineralic composition intercalate with pure olivine layers deformed at intermediate temperatures of about 800–900 °C (Fig. 16c,d and Fig. 17). Like the calcite system, the adaptation of mono- and polymineralic microstructures toward steady-state conditions allows for homogeneous deformation under nearly equiviscous conditions at these deformation temperatures. At even lower temperatures (~700 °C), both dynamic recrystallization and diffusion in olivine are too slow to maintain an efficient dynamic recovery, leading to strain hardening. Consequently, strain localizes in the polymineralic layers deforming under granular flow conditions (Fig. 16e and Fig. 17), while the monomineralic olivine aggregates form isolated rigid lenses (Fig. 16f). Hence, the application of end-member approaches to predicting viscous bulk rheology of polymineralic aggregates (Handy, 1990, 1992; Ji et al., 2003) are limited in cases when switches in the dominant deformation mechanisms occur, which are not defined by the end-member flow behavior (e.g., Bruhn et al., 1999). The bulk strength of a polymineralic mixture can be lower compared to its constituent minerals, especially when granular flow is involved (Wheeler, 1992; Fueten and Robin, 1992; Stünitz and Tullis, 2001; Selverstone and Hyatt, 2003).

The deformation behavior of the two discussed polymineralic systems (calcite-mica and peridotite) suggests that strain localization in polymineralic layers is only important (i) for transient stages with considerable initial variations in grain sizes, or (ii) at low temperatures, where recrystallization and/or diffusion behavior of one of the incorporated phases cannot keep up with the rate of deformation (Fig. 17). In many other cases, however, polymineralic microstructures adapt to deformation such that a steady state is established, for which nearly homogeneous deformation is maintained in the multilayer system (Fig. 17).

9. The role of polymineralic microfabrics in the geodynamic context

There are major differences in processes involved in the evolution of polymineralic microfabrics during static and deformational conditions. As demonstrated above, the resulting microfabrics often result in typical patterns in Zener space at specific physical conditions (compare Figs. 5, 8 and 10, 14). Consequently, polymineralic microfabrics in nature can be used to unravel the geological evolution of rocks in a variety of different geodynamic settings (Fig. 17). Once calibrated, predictions of the microstructural evolution under contact- and regional-metamorphic conditions can be made on the base of grain-size evolution maps (Fig. 14).

In the case of high-strain large-scale shear zones, like continental thrust systems, considerable temperature gradients occur along the transport direction (e.g., Herwegh and Pfiffner, 2005; Ebert et al., 2007b). In this context, grain-size evolution maps can be used to determine spatial temperature gradients. Instead of

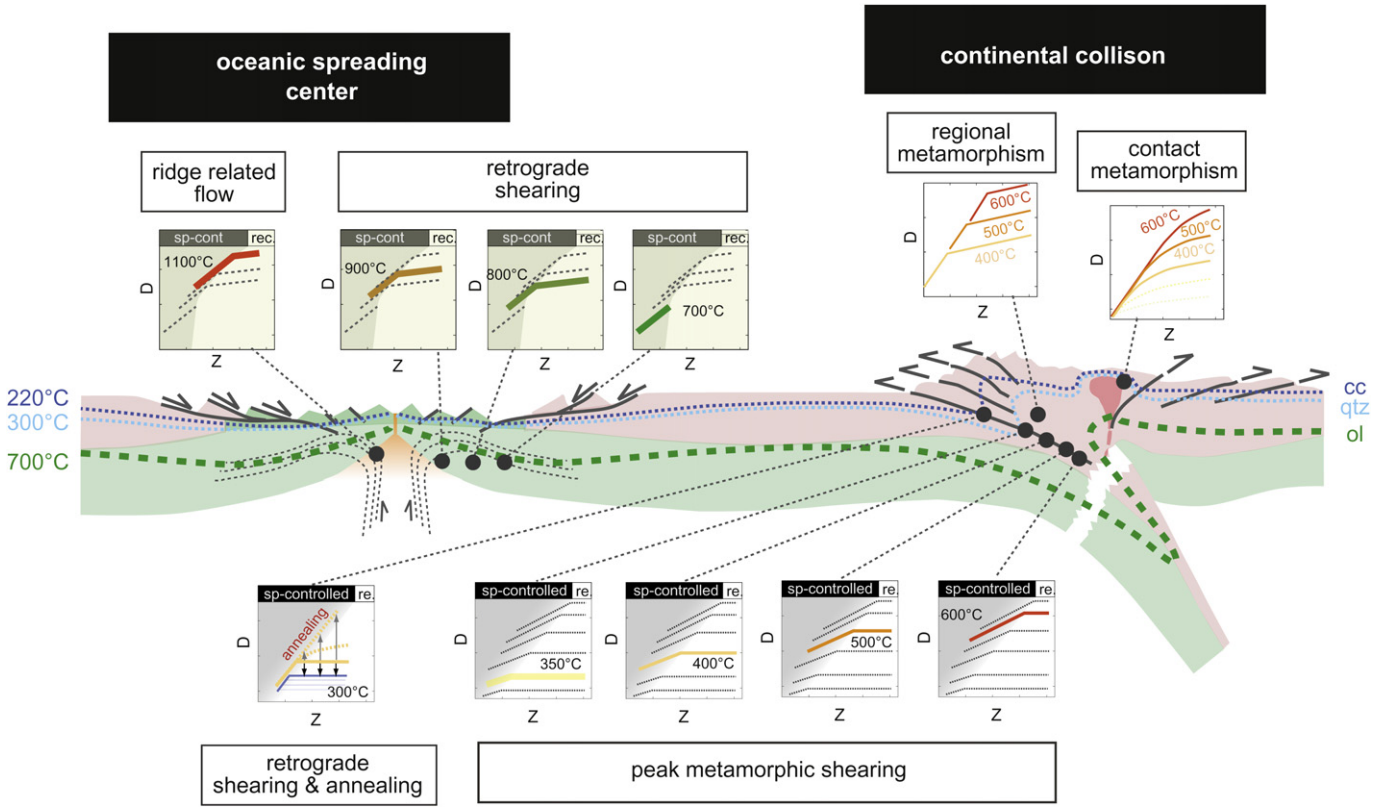

Fig. 17. Occurrence of polymineralic microfabrics in grain size evolution maps in different geodynamic frameworks. Dynamic scenarios like strain localization at mid-ocean ridges or intracontinental fault systems might be unraveled as well as primarily temperature-controlled events like contact or regional metamorphism. As a great advantage, microfabrics frozen in at different time episodes even allow to track down multistage events like the thermal or retrograde deformational overprint of formerly active shear zones (e.g., retrograde shearing and/or annealing). Red: continental lithosphere; green: oceanic crust and lithospheric mantle; orange: asthenospheric mantle with melt percolation. Stippled lines labeled with calcite (cc), quartz (qtz), olivine (ol) indicate the onset of ductile deformation of calcite, quartz and olivine, respectively.

being restricted to monomineralic systems (e.g., Braun et al., 1999; Montesi and Hirth, 2003), grain-size evolution maps can also be used to predict microstructural changes and associated rheologies during strain localization along temperature gradients obtained from numerical models. In this way, the polymineralic nature of the Earth's crust and upper mantle can be accounted for more realistically.

The application of Zener diagrams has great potential for the detection of polystage growth and deformation histories. It is known for a long time that monomineralic microstructures can be overprinted easily, for example, by temperature pulses or static recovery leading to annealing of deformation microstructures by grain growth (Green et al., 1970; Means, 1995; Heilbronner and Tullis, 2002, 2006; Barnhoorn et al., 2005a; Trepmann and Spray, 2006). In contrast, studies of statically overprinted contact-metamorphic polymineralic rocks imply that microstructures with high second-phase content (low Z) are rarely overprinted and preserve grain sizes up to two orders of magnitude smaller than their monomineralic equivalents, even at high temperatures (see Fig. 6). Therefore, polymineralic rocks more likely provide the opportunity to study early microfabrics.

Overprinting relations are common in large-scale shear zones with long-lasting deformation episodes (Means, 1995). Particularly, the preservation potential of type I shear zones (Hull, 1988; Mitra, 1992), where the shear zone widens with increasing deformation, is low. In the opposite case of type II shear zones, characterized by narrowing shear zones, at least the outer regions of the former shear zones may still contain older microfabrics (Means, 1995; Ebert et al., 2007a; Toy et al., 2008; Linckens et al., 2011b). As demonstrated by Herwegh et al. (2008) in the case of retrograde strain localization of carbonate shear zones, earlier high-temperature microfabrics are overprinted close to the tectonic contact of the active shear zone, while older high temperature deformation stages are still preserved in the outer regions of the shear zone (see Fig. 9 in Herwegh et al., 2008). The Zener diagram can be used: (i) to discriminate between the different overprinting steps, (ii) to reconcile older high-temperature microstructures and (iii) to obtain information on earlier deformation conditions. Low-Z regions (microstructures with high second-phase content) should be studied in such cases, because grain boundary migration during annealing may be prevented because of pinning of matrix grains.

By following these approaches, rigorous quantitative studies can be performed to gain insights into the interplay of strain localization and metamorphism for different geodynamic settings ranging from Alpine type continent–continent collisions to classical oceanic rift systems (Fig. 17). The information obtained from the Zener space of a rock's matrix is ideally complemented by studies on porphyroblasts and their inclusions, allowing views far back in geologic time. In combination with geochemical analyses, geophysical measurements/experiments and geochronology, the presented approach provides great potential as analytical tool for the evolution of geodynamic processes.

Acknowledgments

This review article greatly benefited from discussions with many different colleagues over the past couple of years. We would like to thank to all of them, particularly Bjarne Almqvist, Nick Austin, Brian Evans, Luigi Burlini, Uli Faul, Edwin Gnos, Karsten Kunze, Ivan Mercolli, Othmar Müntener, Adrian Pfiffner, and Karl Ramseyer. The constructive reviews of Mark Jessell and Toru Takeshita, as well as the input of Christoph Schrank during the stage of revision, helped to improve the manuscript significantly. We also acknowledge financial support of SNF during the distinct projects carried out over the past decade.

References

Alexander, K.B., Becher, P.F., Waters, S.B., Bleier, A., 1994. Grain growth kinetics in alumina-zirconia (CeZTA) composites. Journal of the American Ceramic Society 77, 939–946.
Ashby, M.F., Verall, R.A., 1973. Diffusion accomodated flow and superplasticity. Acta Metallurgica 21, 149–163.
Austin, N., Evans, B., 2007. Paleowattmeters: a scaling relation for dynamically recrystallized grain size. Geology 35, 343–346.
Austin, N., Evans, B., 2009. The kinetics of microstructural evolution during deformation of calcite. Journal of Geophysical Research-Solid Earth 114.
Austin, N., Evans, B., Herwegh, M., Ebert, A., 2008. Strain localization in the Morcles nappe (Helvetic Alps, Switzerland). Swiss Journal of Geosciences 101, 341–360.
Barnhoorn, A., Bystricky, M., Burlini, L., Kunze, K., 2004. The role of recrystallisation on the deformation behaviour of calcite rocks: large strain torsion experiments on Carrara marble. Journal of Structural Geology 26, 885–903.
Barnhoorn, A., Bystricky, M., Burlini, L., Kunze, K., 2005a. Post-deformational annealing of calcite rocks. Tectonophysics 403, 167–191.
Barnhoorn, A., Bystricky, M., Kunze, K., Burlini, L., Burg, J.P., 2005b. Strain localisation in bimineralic rocks: experimental deformation of synthetic calcite-anhydrite aggregates. Earth and Planetary Science Letters 240, 748–763.
Berger, A., Herwegh, M., 2004. Grain coarsening of contact metamorphic carbonates: effects of second phase particles, fluid flow and thermal perturbations. Journal of Metamorphic Geology 22, 459–474.
Berger, A., Stünitz, H., 1996. Deformation mechanisms and reaction of hornblende: examples from the Bergell tonalite (Central Alps). Tectonophysics 257, 149–174.
Berger, A., Brodhag, S., Herwegh, M., 2010. Reaction-induced nucleation and growth versus grain coarsening in contact metamorphic, impure carbonates. Journal of Metamorphic Geology 28, 809–824.
Berger, A., Herwegh, M., Putlitz, B., Schwarz, O.J. in this volume. Quantitative analysis of crystal/grain sizes and their distributions. Journal of Structural Geology.
Bestmann, M., Kunze, K., Matthews, A., 2000. Evolution of a calcite marble shear zone complex on Thassos Island, Greece: microstructural and textural fabrics and their kinematic significance. Journal of Structural Geology 22, 1789–1807.
Biot, M.A., 1961. Theory of Folding of Stratified Viscoelastic Media and its Implications in Tectonics and Orogenesis. In: Geological Society of America Bulletin, 72 1595–1620.
Braun, J., Chéry, J., Poliakov, A.N.B., Mainprice, D., Vauchez, A., Tommasi, A., Daignières, M., 1999. A simple parameterization of strain localization in the ductile regime due to grain size reduction. Journal of Geophysical Research 104, 25167–25181.
Brodhag, S.H., Herwegh, M., 2010. The effect of different second-phase particle regimes on grain growth in two-phase aggregates: insights from in situ rock analogue experiments. Contributions to Mineralogy and Petrology 160, 219–238.
Brodhag, S.H., Herwegh, M., Berger, A., 2011. Grain coarsening in polymineralic contact metamorphic carbonate rocks: the role of different physical interactions during coarsening. Journal of Structural Geology 33, 689–712.
Bruhn, D.F., Olgaard, D.L., Dell'Angelo, L.N., 1999. Evidence for enhanced deformation in two-phase rocks: experiments on the rheology of calcite-anhydrite aggregates. Journal of Geophysical Research 104, 707–724.
Brunner, W.M., 1984. Crack growth during unroofing of crustal rocks: effects on thermoelastic behavior and near-surface stresses. Journal of Geophysical Research 89, 4167–4184.
Burg, J.P., Wilson, C.J.L., 1987. Deformation of two-phase systems with contrasting litholgies. Tectonophysics 135, 199–205.
Cahn, J.W., 1962. Impurity-drag effect in grain boundary motion. Acta Metallurgica 10, 789–798.
Carlson, W.D., Denison, C., 1992. Mechanisms of porphyroblast crystallization – results from high-resolution computed x-ray tomography. Science 257, 1236–1239.
Carlson, W.D., Gordon, C.L., 2004. Effects of matrix grain size on the kinetics of intergranular diffusion. Journal of Metamorphic Geology 22, 733–742.
Covey-Crump, S.J., 1997. The normal grain growth behavior of nominally pure calcitic aggregates. Contributions to Mineralogy and Petrology 129, 239–254.
Davies, N.E., Newman, J., Wheelock, P.B., Kornenberg, A.K., 2010. Grain growth kinetics of dolomite, magnesite and calcite: a comparitive study. Physics and Chemistry of Minerals 38, 123–138.
de Bresser, J., Peach, C., Reijs, J., Spiers, C., 1998. On dynamic recrystallization during solid state flow: effects of stress and temperature. Geophysical Research Letters 25, 3457–3460.
de Bresser, J.H.P., ter Heege, J.H., Spiers, C.J., 2001. Grain size reduction by dynamic recrystallization: can it result in major rheological weakening? The International Journal of Earth Sciences (Geologische Rundschau) 90, 28–45.
de Ronde, A.A., Stünitz, H., Tullis, J., Heilbronner, R., 2005. Reaction-induced weakening of plagioclase-olivine composites. Tectonophysics 409, 85–106.
Delle Piane, C., Wilson, C.J.L., Burlini, L., 2009. Dilatant plasticity in high-strain experiments on calcite-muscovite aggregates. Journal of Structural Geology 31, 1084–1099.

Dimanov, A., Dresen, G., 2005. Rheology of synthetic anorthite-diopside aggregates: implications for ductile shear zones. Journal of Geophysical Research-Solid Earth 110.
Doherty, R.D., Hughes, D.A., Humphreys, F.J., Jonas, J.J., Jensen, J.D., Kassner, M.E., King, W.E., McNelley, T.R., McQueen, H.J., Rollett, A.D., 1997. Current issues in recrystallization: a review. Material Science and Engineering A238, 219–274.
Dresen, G., Evans, B., 1993. Brittle and semibrittle deformation of synthetic marbles Composed of two phases. Journal of Geophysical Research 98, 11921–11933.
Dresen, G., Evans, B., Olgaard, D.L., 1998. Effect of quartz inclusions on plastic flow in marble. Geophysical Research Letters 25, 1245–1248.
Drury, M.R., Urai, J.L., 1990. Deformation-related recrystallization processes. Tectonophysics 172, 235–253.
Dunlap, W.J., Hirth, G., Teyssier, C., 1997. Thermomechanical evolution of a ductile duplex. Tectonics 16, 983–1000.
Ebert, A., Herwegh, M., Pfiffner, O.A., 2007a. Cooling induced strain localization in carbonate mylonites within a large-scale shear zone (Glarus thrust, Switzerland). Journal of Structural Geology 29, 1164–1184.
Ebert, A., Herwegh, M., Austin, N., Evans, B., Pfiffner, O.A., 2007b. Microfabrics in carbonate mylonites along a large-scale shear zone (Helvetic Alps). Tectonophysics 444, 1–26.
Ebert, A., Herwegh, M., Berger, A., Pfiffner, O.A., 2008. Grain coarsening maps for polymineralic carbonate mylonites: a calibration based on data from different Helvetic nappes (Switzerland). Tectonophysics 457, 128–142.
Escartin, J., Hirth, G., Evans, B., 2001. Strength of slightly serpentinized peridotites: implications for the tectonics of oceanic lithosphere. Geology 29, 1023–1026.
Etheridge, M.A., Wilkie, J.C., 1979. Grainsize reduction, grain boundary sliding and flow strength of mylonites. Tectonophysics 58, 159–178.
Evans, B., Renner, J., Hirth, G., 2001. A few remarks on the kinetics of static grain growth in rocks. The International Journal of Earth Sciences (Geologische Rundschau) 90, 88–103.
Farver, J.R., Yund, R.A., 1996. Volume and grain boundary diffusion of calcium in natural and hot-pressed calcite aggregates. Contributions to Mineralogy and Petrology 123, 77–91.
Farver, J.R., Yund, R.A., 1998. Oxygen grain boundary diffusion in natural and hot-pressed calcite aggregates. EPSL 161, 189–200.
Fischer, M.P., Woodward, N.B., 1992. The geometrical evolution of foreland thrust systems. In: McClay, K.R. (Ed.), Thrust Tectonics. Chapman and Hall, London, pp. 181–189.
Fitz Gerald, J.D., Stunitz, H., 1993. Deformation of granitoids at low metamorphic grade. 1. Reactions and grain-size reduction. Tectonophysics 221, 269–297.
Fliervoet, T.F., White, S.T., 1995. Quartz deformation in a very fine grained quartzo-feldspathic mylonite: a lack of evidence for dominant grain boundary sliding deformation. Journal of Structural Geology 17, 1095–1109.
Frederich, J.T., Wong, T.F., 1986. Micromechanics of thermally induced cracking in three crustal rocks. Journal of Geophysical Research 91, 12743–12764.
Freund, D., Rybacki, E., Dresen, G., 2001. Effect of impurities on grain growth in synthetic calcite aggregates. Phys. Chem. Minerals 28, 737–745.
Frost, H.J., Ashby, M.F., 1982. Deformation Mechnism Maps. Pergamon Press, Toronto. 1–166.
Fueten, F., Robin, P.Y.F., 1992. Finite-element modeling of the propagation of a pressure solution cleavage seam. Journal of Structural Geology 14, 953–962.
Fusseis, F., Handy, M.R., Schrank, C., 2006. Networking of shear zones at the brittle-to-viscous transition (Cap de Creus, NE Spain). Journal of Structural Geology 28, 1228–1243.
Fusseis, F., Regenauer-Lieb, K., Lui, J., Hough, R.M., De Carlo, F., 2009. Creep cavitation can establish a dynamic granular fluid pump in ductile shear zone. Nature 459, 974–977.
Gladman, T., 1966. On the theory of the effect of precipitates in solutions. Proceedings of the Royal Society of London 294A, 298–309.
Gleason, G.C., Tullis, J., Feidelbach, F., 1993. The role of dynamic recrystallization in the development of lattice preferred orientations in experimentally deformed quartz aggregates. Journal of Structural Geology 15, 1145–1168.
Gottstein, G., Molodov, D.A., Shvindlerman, L.S., 2006. Kinematics, dynamics, and microstructural effects of grain boundary junctions. Journal of Materials Science 41, 7730–7740.
Green, H.W., Griggs, D.T., Christie, J.M., 1970. Syntectonic and Annealing Recrystallization of Fine-grained Quartz Aggregates. Springer, New York.
Guillopé, M., Poirier, J.P., 1979. Dynamic recrystallization during creep of single-crystalline halite: an experimental study. Journal of Geophysical Research 84, 5557–5567.
Grujic, D., Stipp, M., Wooden, J.L., 2009. Thermometry of quartz mylonites. Geochimica Et Cosmochimica Acta 73 (13) A472–A472.
Handy, M.R., 1987. The structure, age and kinematics of the Pogallo fault zone; southern Alps, northwestern Italy. Eclogae Geologicae Helvetiae 80, 593–632.
Handy, M.R., 1989. Deformation regimes and the rheological evolution of fault zones in the lithosphere: the effects of pressure, temperature, grain size and time. Tectonophysics 163, 119–152.
Handy, M.R., 1990. The solid-state flow of polymineralic rocks. Journal of Geophysical Research 95, 8647–8661.
Handy, R.M., 1992. Correction and addition to "The solid-state flow of polymineralic rocks". Journal of Geophysical Research 97, 1897–1899.
Handy, M.R., 1994. Flow laws for rocks containing two non-linear viscous phases: a phenomenological approach. Journal of Structural Geology 16, 287–301.
Hay, R.S., Evans, B., 1987. Chemically induced grain boundary migration in calcite: temperature dependence, phenomenology, and possible applications to geologic systems. Contributions to Mineralogy and Petrology 97, 127–141.
Heilbronner, R., Tullis, J., 2002. The effect of static annealing on microstructures and crystallographic preferred orientations of quartzites experimentally deformed in axial compression. In: de Meer, S., Drury, M.R., de Bresser, J.H.P., Pennock, G.M. (Eds.), Deformation Mechanisms, Rheology and Tectonics: Current Status and Future Perspectives. Geological Society, London, pp. 191–218.
Heilbronner, R., Tullis, J., 2006. Evolution of c axis pole figures and grain size during dynamic recrystallization: results from experimentally sheared quartzite. Journal of Geophysical Research-Solid Earth 111, 191–218.
Herwegh, M., Berger, A., 2003. Differences in grain growth of calcite: a field-based modeling approach. Contributions to Mineralogy and Petrology 145, 600–611.
Herwegh, M., Berger, A., 2004. Deformation mechanisms in second-phase affected microstructures and their energy balance. Journal of Structural Geology 26, 1483–1498.
Herwegh, M., Handy, M.R., 1998. The origin of shape preferred orientation in mylonite: inferences from in-situ experiments on polycrystalline norcamphor. Journal of Structural Geology 20, 681–694.
Herwegh, M., Jenni, A., 2001. Granular flow in polymineralic rocks bearing sheet silicates: new evidences from natural examples. Tectonophysics 332, 309–320.
Herwegh, M., Pfiffner, O.A., 2005. Tectono-metamorphic evolution of a nappe stack: a case study of the Swiss Alps. Tectonophysics 404, 55–76.
Herwegh, M., Xiao, X., Evans, B., 2003. The effect of dissolved magnesium on diffusion creep in calcite. EPSL 212, 457–470.
Herwegh, M., Berger, A., Ebert, A., 2005a. Grain coarsening maps: a new tool to predict microfabric evolution of polymineralic rocks. Geology 33, 801–804.
Herwegh, M., de Bresserter Heege, J.H.P., ter Heege, J.H., 2005b. Combining natural microstructures with composite flow laws: an improved approach for the extrapolation of lab data to nature. Journal of Structural Geology 27, 503–521.
Herwegh, M., Berger, A., Ebert, A., Brodhag, S., 2008. Discrimination of annealed and dynamic fabrics: consequences for strain localization and deformation episodes of large-scale shear zones. Earth and Planetary Science Letters 276, 52–61.
Herwegh, M., Handy, M.R., 1996. The evolution of high temperature mylonitic microfabrics: evidence from simple shearing of a quartz analogue (norcamphor). Journal of Structural Geology 18, 689–710.
Higgins, G.T., Wiryolukito, S., Nash, P., 1992. The kinetics of coupled phase coarsening in two-phase structures. Materials Science Forum 94–96, 671–676.
Hillert, M., Purdy, G.R., 1978. Chemically induced grain boundary migration. Acta Metall 26, 333–340.
Hiraga, T., Tachibana, C., Ohashi, N., Sano, S., 2010. Grain growth systematics for forsterite±enstatite aggregates: effect of lithology on grain size in the upper mantle. Earth and Planetary Science Letters 291, 10–20.
Hirsch, D.M., Carlson, W.D., 2006. Variations in rates of nucleation and growth of biotite porphyroblasts. Journal of Metamorphic Geology 24, 763–777.
Hirth, G., Tullis, J., 1992. Dislocation creep regimes in quartz aggregates. Journal of Structural Geology 14, 145–159.
Hobbs, B.E., 1966. Microfabric of tectonites from Wyangala dam area New South Wales Australia. In: Geological Society of America Bulletin, vol. 77 685–706.
Holyoke, C.W., Tullis, J., 2006a. Formation and maintenance of shear zones. Geology 34, 105–108.
Holyoke, C.W., Tullis, J., 2006b. The interaction between reaction and deformation: an experimental study using a biotite plus plagioclase plus quartz gneiss. Journal of Metamorphic Geology 24, 743–762.
Hudleston, P.J., 1980. The progressive development of inhomogenous shear and crystallographic fabrics in glacial ice. Journal of Structural Geology 2, 189–196.
Hull, J., 1988. Thickness-displacement relationships for deformation zones. Journal of Structural Geology 10, 431–435.
Jaroslow, G.E., Hirth, G., Dick, H.J.B., 1996. Abyssal peridotite mylonites: implications for grain-size sensitive flow and strain localization in the oceanic lithosphere. Tectonophysics 256, 17–37.
Jerram, D.A., Higgins, M.D., 2007. 3D analysis of rock textures: quantifying igneous microstructures. Elements 3, 239–245.
Jerram, D.A., Cheadle, M.J., Hunter, R.H., Elliott, M.T., 1996. The spatial distribution of grains and crystals in rocks. Contributions to Mineralogy and Petrology 125, 60–74.
Jessell, M.W., Kostenko, O., Jamtveit, B., 2003. The preservation potential of microstructures during static grain growth. Journal of Metamorphic Geology 21, 481–491.
Ji, S., Wang, Z., Wirth, R., 2001. Bulk flow strength of forsterite-enstatite composites as a function of forsterite content. Tectonophysics 341, 69–93.
Ji, S., Zhao, P., Xia, B., 2003. Flow laws of multiphase materials and rocks from end-member flow laws. Tectonophysics 370, 129–154.
Joesten, R.L.J., 1983. Grain growth and grain boundary diffusion in quartz from Christmas Mountain (Texas) contact aureole. American Journal of Science 283A, 233–254.
Joesten, R.L.J., 1991. Kinetics of coarsening and diffusion-controlled mineral growth. In: Kerrick, D.M. (Ed.), Contact Metamorphism, pp. 507–582.
Jordan, P.G., 1987. The deformation behavior of bimineralic limestone-halite aggregates. Tectonophysics 147, 185–197.
Karato, S., 1989. Grain growth kinetics in olivine aggregates. Tectonophysics 168, 255–273.
Kenkmann, T., Dresen, G., 2002. Dislocation microstructure and phase distribution in a lower crustal shear zone - an example from the Ivrea-Zone, Italy. International Journal of Earth Sciences 91, 445–458.
Kohlstedt, D.L., Evans, B., Mackwell, S.J., 1995. Strength of the lithosphere-constraints imposed by laboratory experiments. Journal Of Geophysical Research 100 (B9), 17587–17602.

Krabbendam, M., Urai, J.L., van Vliet, L.J., 2003. Grain size stabilization by dispersed graphite in a high-grade quartz mylonite: an example from Naxos (Greece). Journal of Structural Geology 25, 855–866.
Kruse, R., Stünitz, H., 1999. Deformation mechanisms and phase distribution in mafic high-temperature mylonites from the Jotun Nappe, southern Norway. Tectonophysics 303, 223–249.
Linckens, J., 2010. Microfabric Evolution and Strain Localization in the Naturally Deformed Mantle Rocks. PhD thesis University of Bern. 160pp.
Linckens, J., Herwegh, M., Muentener, O., 2011a. Linking temperature estimates and microstructures in deformed polymineralic mantle rocks. Gcubed 12, 1–19.
Linckens, J., Herwegh, M., Muntener, O., Mercolli, I., 2011b. Evolution of a polymineralic mantle shear zone and the role of second phases on the localization of deformation. Journal of Geophysical Research 116, B06210.
Liu, J., Regenauer-Lieb, K., Hines, C., Liu, K., Gaede, O., Squelch, A., 2009. Improved estimates of percolation and anisotropic permeability from 3-D X-ray microtomography using stochastic analyses and visualization. Geochemistry Geophysics Geosystems 10, 2–13.
Mancktelow, N.S., Pennacchioni, G., 2004. The influence of grain boundary fluids on the microstructure of quartz-feldspar mylonites. Journal of Structural Geology 26, 47–69.
Manohar, P.A., Ferry, M., Chandra, T., 1998. Five decades of the Zener equation. ISIJ International 38, 913–924.
Mas, D.L., Crowley, P.D., 1996. The effect of second-phase particles on stable grain sizes in regionally metamorphosed polyphase calcite marbles. Journal of Structural Geology 14, 155–162.
McCaig, A., Covey-Crump, S.J., Ben Ismail, W., Lloyd, G.E., 2007. Fast diffusion along mobile grain boundaries in calcite. Contributions to Mineralogy and Petrology 153.
Means, W.D., 1976. Stress and Strain. Springer-Verlag, New York.
Means, W.D., 1981. The concept of steady-state foliation. Tectonophysics 78, 179–199.
Means, W., 1995. Shear zones and rock history. Tectonophysics 247, 157–160.
Mehl, L., Hirth, G., 2008. Plagioclase preferred orientation in layered mylonites: evaluation of flow laws for the lower crust. Journal of Geophysical Research 113, 1–19.
Mitra, G., 1992. Deformation of granitic basement rocks along fault zones at shallow to intermediate crustal levels. In: Mitra, S., Fisher, G.W. (Eds.), Structural Geology of Fold and Thrust Belts. Johns Hopkins University Press, Baltimore, pp. 123–144.
Montesi, L.G.J., Hirth, G., 2003. Grain size evolution and the rheology of ductile shear zones: from laboratory experiments to postseismic creep. Earth and Planetary Science Letters 211, 97–110.
Muller, T., Baumgartner, L.P., Foster, C.T., Bowman, J.R., 2009. Crystal size distribution of Periclase in contact metamorphic dolomite marbles from the southern Adamello massif, Italy. Journal of Petrology 50, 451–465.
Nes, E., Ryum, N., Hunderi, O., 1985. On the Zener drag. Acta Metallurgica 33, 11–22.
Newman, J., Lamb, W.M., Drury, M.R., Vissers, R.L.M., 1999. Deformation processes in a peridotite shear zone: reaction-softening by an H2O-deficient, continuous net transfer reaction. Tectonophysics 303, 193–222.
Oesterling, N., Heilbronner, R., Stunitz, H., Barnhoorn, A., Molli, G., 2007. Strain dependent variation of microstructure and texture in naturally deformed Carrara marble. Journal of Structural Geology 29, 681–696.
O'Hara, K., 2007. Reaction weakening and emplacement of crystalline thrusts: diffusion control on reaction rate and strain rate. Journal of Structural Geology 29, 1301–1314.
Okudaira, T., Ogawa, D., Michibayashi, K., 2010. Grain-size-sensitive deformation of upper greenschist- to lower amphibolite-facies metacherts. Tectonophysics 492, 141–149.
Olgaard, D.L., 1990. The role of second phase in localizing deformation. In: Knipe, R.J., Rutter, E.H. (Eds.), Deformation Mechanisms, Rheology and Tectonics. Geological Society Special Publication, pp. 175–181.
Olgaard, D.L., Evans, B.E., 1986. Effect of second-phase particles on grain growth in calcite. Journal of the American Ceramic Society 69, C272–C277.
Olgaard, D.L., Evans, B., 1988. Grain growth in synthetic marbles with added mica and water. Contributions to Mineralogy and Petrology 100, 246–260.
Passchier, C.W., Trouw, R.A.J., 2005. Microtectonics. Springer-Verlag Berlin Heidelberg, New York.
Paterson, M.S., 1995. A theory of granular flow accommodated by material transfer via intergranular fluid. Tectonophysics 245, 135–151.
Pearce, M.A., Wheeler, J., 2010. Modelling grain-recycling zoning during metamorphism. Journal of Metamorphic Geology 28, 423–437.
Piazolo, S., Sursaeva, V.G., Prior, D.J., 2005. The influence of triple junction kinetics on the evolution of polycrystalline materials during normal grain growth: new evidence from in-situ experiments using columnar Al foil. Zeitschrift Für Metallkunde 96, 1152–1157.
Pieri, M., Burlini, L., Kunze, K., Stretton, I., Olgaard, D.L., 2001. Rheological and microstructural evolution of Carrara marble with high shear strain: results from high temperature torsion experiments. Journal of Structural Geology 23, 1393–1413.
Poirier, J.P., Guillopé, M., 1979. Deformation induced recrystallization of minerals. Bulletin Mineral 102, 67–74.
Ramsay, J.G., 1967. Folding and Fracturing of Rocks. Mc-Graw-Hill, New York, NY.
Ramsay, J.G., 1980. Shear zone geometry: a review. Journal of Structural Geology 2, 83–99.
Ree, J.H., 1991. An experimental steady-state foliation. Journal of Structural Geology 13, 1001–1011.
Ree, J.H., 1994. Grain boundary sliding and development of grain boundary openings in experimentally deformed octachloropropane. Journal of Structural Geology 16, 403–418.
Regenauer-Lieb, K., Yuen, D.A., 2003. Modeling shear zones in geological and planetary sciences: solid- and fluid-thermal-mechanical approaches. Earth-Science Reviews 63, 295–349.
Renner, J., Siddiqi, G., Evans, B., 2007. Plastic flow of two-phase marbles. Journal of Geophysical Research-Solid Earth 112, 1–16.
Ricard, Y., Bercovici, D., 2009. A continuum theory of grain size evolution and damage. Journal of Geophysical Research 114, B01204.
Rosenberg, C.L., Handy, M.R., 2005. Experimental deformation of partially melted granite revisited: implications for the continental crust. Journal of Metamorphic Geology 23, 19–28.
Rutter, E.H., 1995. Experimental study of the influence of stress, temperature, and strain on the dynamic recrystallization of Carrara marble. Journal of Geophysical Research 100, 24651–24663.
Rutter, E.H., Brodie, K.H., 1988. Experimental syntectonic dehydration of serpentinite under conditions of controlled pore water pressure. Journal of Geophysical Research 93, 4907–4932.
Rybacki, E., Paterson, M.S., Wirth, R., Dresen, G., 2003. Rheology of calcite-quartz aggregates deformed to large strain in torsion. Journal of Geophysical Research-Solid Earth 108.
Rybacki, E., Wirth, R., Dresen, G., 2008. High-strain creep of feldspar rocks: implications for cavitation and ductile failure in the lower crust. Geophysical Research Letters 35, L04304.
Ryum, N., Hunderi, O., Nes, E., 1983. On grain boundary drag from second phase particles. Scripta Metallurgica 17, 1281–1283.
Schmid, J., 1997. The Genesis of White Marbles: Geological Cause and Archeological Applications, Bern, p. 156.
Schmid, S.M., Handy, M.R., 1991. Towards a genetic classification of fault rocks: geological usage and tectonophysical implications. In: Müller, D.W., McKenzie, J.A., Weissert, H. (Eds.), Contoversies in Modern Geology. Academic Press, London, pp. 95–110.
Schrank, C.E., Handy, M.R., Fusseis, F., 2008a. Multiscaling of shear zones and the evolution of the brittle-to-viscous transition in continental crust. Journal of Geophysical Research 113.
Schrank, C.E., Boutelier, D.A., Cruden, A.R., 2008b. The analogue sehar zone: from rheology to associated geometry. Journal of Structural Geology 30, 177–193.
Selverstone, J., Hyatt, J., 2003. Chemical and physical responses to deformation in micaceous quartzites from the Tauern Window, Eastern Alps. Journal of Metamorphic Geology 21, 335–345.
Shimizu, I., 1998. Stress and temperature dependence of recrystallized grain size: a subgrain misorientation model. Geophysical Research Letters 25, 4237–4240.
Skemer, P., Warren, J.M., Kelemen, P.B., Hirth, G., 2010. Microstructural and rheological evolution of a mantle shear zone. Journal of Petrology 51, 43–53.
Smith, C.S., 1948. Grains, phases, and interphases: an interpretation of microstructure. Transactions of the American Institute of Mining and Metallurgical Engineers 175, 15–51.
Song, W.J., Ree, J.H., 2007. Effect of mica on the grain size of dynamically recrystallized quartz in a quartz-muscovite mylonite. Journal of Structural Geology 29, 1872–1881.
Spear, F.S., 1993. Metamorphic Phase Equilibria and Pressure-Temperature-Time Paths. In: Mineralogical Society of America Monograph, 799 pp.
Stünitz, H., Fitz Gerald, J.D., 1993. Deformation of granitoids at low metamorphic grade II. Granular flow in albite-rich mylonites. Tectonophysics 221, 299–324.
Stünitz, H., 1998. Syndeformational recrystallization: dynamic or compositionally induced? Contributions to Mineralogy and Petrology 131, 219–236.
Stünitz, H., Tullis, J., 2001. Weakening and strain localization produced by syndeformational reaction of plagioclase. The International Journal of Earth Sciences (Geologische Rundschau) 90, 136–148.
Stipp, M., Stünitz, H., Heilbronner, R., Schmid, S.M., 2002a. Dynamic recrystallization of quartz: correlation between natural and experimental conditions. In: de Meer, S., Drury, M.R., de Bresser, J.H.P., Pennock, G.M. (Eds.), Deformation Mechanisms, Rheology and Tectonics: Current Status and Future Perspectives. Geological Society, London, pp. 171–190. Special Publications 200.
Stipp, M., Stünitz, H., Heilbronner, R., Schmid, S.M., 2002b. The eastern Tonale fault zone: a 'natural laboratory' for crystal plastic deformation of quartz over a temperature range from 250 to 700°C. Journal of Structural Geology 24, 1861–1884.
Stipp, M., Tullis, J., Scherwath, M., Behrmann, J.H., 2010. A new perspective on paleopiezometry: dynamically recrystallized grain size distributions indicate mechanism changes. Geology 38, 759–762.
ter Heege, J.H., de Bresser, J.H.P., Spiers, C.J., 2002. The influence of dynamic recrystallization on the grain size distribution and rheological behavior of Carrara marble deformed in axial compression. In: de Meer, S., Drury, M.R., de Bresser, J.H.P., Pennock, G.M. (Eds.), Deformation Mechanisms, Rheology and Tectonics: Current Status and Future Perspectives. Geological Society of London, pp. 331–353.
Toy, V.G., Prior, D.J., Norris, R.J., 2008. Quartz fabrics in the Alpine Fault mylonites: influence of pre-existing preferred orientations on fabric development during progressive uplift. Journal of Structural Geology 30, 602–621.
Toy, V.G., Newman, J., Lamb, W., Tikoff, B., 2009. The role of pyroxenites in formation of shear instabilities in the mantle: evidence from an ultramafic ultramylonite, Twin Sisters Massif, Washington. Journal of Petrology 51, 55–80.

Trepmann, C.A., Spray, J.G., 2006. Shock-induced crystal-plastic deformation and post-shock annealing of quartz: microstructural evidence from crystalline target rocks of the Charlevoix impact structure, Canada. European Journal of Mineralogy 18, 161–173.
Tullis, T.E., Horowitz, F.G., Tullis, J., 1991. Flow laws of polyphase aggregates from end-member flow laws. Journal of Geophysical Research 96, 8081–8096.
Turner, F.J., Weiss, L.E., 1963. Structural Analysis of Metamorphic Tectonites. McGraw Hill, New York.
Twiss, R.J., 1977. Theory and applicability of a recrystallized grain size paleopiezometer. Pure and Applied Geophysics 115, 227–244.
Urai, J.L., Means, W.D., Lister, G.S., 1986. Dynamic recrystallization of minerals. In: Heard, H.C., Hobbs, B.E. (Eds.), Mineral and Rock Deformation: Laboratory Studies – the Paterson Volume. American Geophysical Union Monographs, vol. 36, pp. 161–199.
van Daalen, M., Heilbronner, R., Kunze, K., 1999. Orientation analysis of localized shear deformation in quartz fibres at the brittle-ductile transition. Tectonophysics 303, 83–107.
Vanderwal, D., Chopra, P., Drury, M., Fitz Gerald, J.D., 1993. Relationships between dynamically recrystallized grain-size and deformation conditions in experimentally deformed olivine rocks. Geophysical Research Letters 20, 1479–1482.
Vernon, R.H., 2004. A Practical Guide to Rock Microstructure. University Press Cambridge, Cambridge. 394pp.
Vernooij, M.G.C., den Brok, B., Kunze, K., 2006. Development of crystallographic preferred orientations by nucleation and growth of new grains in experimentally deformed quartz single crystals. Tectonophysics 427, 35–53.
Voll, G., 1960. New work on petrofabrics. Liverpool and Manchester. Geological Journal 2, 503–567.
Warren, J.M., Hirth, G., 2006. Grain size sensitive deformation mechanisms in naturally deformed peridotites. Earth and Planetary Science Letters 248, 438–450.
Watts, M.J., Williams, G.D., 1983. Strain geometry, microstructure and mineral chemistry in metagabbro shear zones – a study of softening mechanisms during progressive mylonitization. Journal of Structural Geology 5, 507–517.
Wheeler, J., 1992. Importance of pressure solution and coble creep in the deformation of polymineralic rocks. Journal of Geophysical Research-Solid Earth 97, 4579–4586.
White, S.H., Burrows, S.E., Carreras, J., Shaw, N.D., Humphreys, F.J., 1980. On mylonites in ductile shear zones. Journal of Structural Geology 2, 175–187.
Wilson, C.J.L., Evans, L., Delle Piane, C., 2009. Modelling of porphyroclasts in simple shear and the role of stress variations at grain boundaries. Journal of Structural Geology 31, 1350–1364.
Wintsch, R.P., Christoffersen, R., Kronenberg, A.K., 1995. Fluid-rock reaction weakening of fault zones. Journal of Geophysical Research-Solid Earth 100, 13021–13032.
Xiao, X.H., Evans, B., 2003. Shear-enhanced compaction during non-linear viscous creep of porous calcite-quartz aggregates. Earth and Planetary Science Letters 216, 725–740.
Zu, W., Gaetani, G.A., Fusseis, F., Montési, L.G.J., De Carlo, F., 2011. Microtomography of partially molten rocks: three-dimensional melt distribution in mantle peridotite. Sciences 332, 88–91.